

## A COMPREHENSIVE CHARACTERIZATION OF DIOCTAHEDRAL SMECTITES

FELICITAS WOLTERS<sup>1,\*,\ddagger</sup>, GERHARD LAGALY<sup>2</sup>, GUENTER KAHR<sup>3</sup>, ROLF NUESCH<sup>†</sup>, AND KATJA EMMERICH<sup>1,4</sup>

<sup>1</sup> Institute for Technical Chemistry, Water and Geotechnology Division, Forschungszentrum Karlsruhe GmbH, P.O. Box 3640, 76021 Karlsruhe, Germany

<sup>2</sup> Institute of Inorganic Chemistry, University of Kiel, D-24098 Kiel, Germany

<sup>3</sup> ETH Zurich, Institute for Geotechnical Engineering, Schafmattstr. 6, 8093 Zürich, Switzerland

<sup>4</sup> Competence Center for Material Moisture, University of Karlsruhe, c/o Forschungszentrum Karlsruhe, ITC-WGT, P.O. Box 3640, 76021 Karlsruhe, Germany

**Abstract**—The term ‘montmorillonite’ encompasses a wide range of chemical compositions and structures. Comprehensive and reliable characterization is essential for unambiguous classification. Twenty eight purified, Na-exchanged smectites (<0.2  $\mu\text{m}$ ) were characterized by layer-charge measurement using the alkylammonium method, by cation exchange capacity (CEC) measurement with Cu-triethylenetetramine, by determination of the chemical composition using X-ray fluorescence analysis, by calculation of the structural formula following determination of the octahedral structure (*trans*-vacant vs. *cis*-vacant) by simultaneous thermal analysis, and by X-ray diffraction analysis. Mössbauer spectroscopy was applied to determine the oxidation state and coordination of Fe and changes thereof during purification of the source materials.

The charge derived from chemical composition was considerably greater (by up to 30%) than the measured layer charge. The independently measured layer charge was used to calculate the structural formula. The measured CEC values, comprising the permanent charges and the pH-dependent edge charges, were consistent with measured layer charge but not with layer charge derived from the chemical composition. Therefore, the structural formula of smectites should be calculated using the measured layer charge.

The dehydroxylation temperature, which conveys information about the structure of the octahedral sheet, was correlated to the amount of Mg and Fe<sup>3+</sup> and the location of charges. No relationship was found among the dehydroxylation temperature and the mean layer charge or the Mg content. In contrast, a clear relationship was observed between the Fe content and the dehydroxylation temperature. Montmorillonites with an Fe content <0.3/f.u. are *cis*-vacant and those containing Fe<sup>3+</sup> > 0.3 mol/f.u. are *trans*-vacant, mostly with additional *cis*-vacancies. Tetrahedral substitution also appeared to be a function of the number of *trans*-vacancies.

The parameters analyzed provide the basis for a new descriptive classification system.

**Key Words**—CEC, Chemical Composition, *Cis*-vacant, Dehydroxylation, Fe content, Layer Charge, Montmorillonite, Octahedral Charge, Simultaneous Thermal Analysis, Structural Formula, Tetrahedral Charge, *Trans*-vacant.

### INTRODUCTION

Bentonites vary widely in terms of their texture and their mineralogical and chemical compositions. The structure of the smectites in bentonites is important in terms of the properties and various applications of these swelling clays. Different applications such as geotechnical barriers in radioactive-waste disposal, in clay-polymer-nanocomposites, or in molding sands in foundries need different types of bentonite. In industrial applications, index tests such as methylene-blue adsorption or chemical composition are used to define quality. Saving time on analyses is good but explaining

unexpected poor performance or even failures of materials can be time-consuming and expensive. An unambiguous classification should allow a better understanding of the structure-functionality relationship.

The feasibility of the proposed classification of montmorillonites (Emmerich *et al.*, 2009) is discussed here, focusing mainly on montmorillonites and a few beidellites.

Different types of montmorillonite were identified by Grim and Kulbicki (1961), Schultz (1969), Brigatti and Poppi (1981), and Brigatti (1983). They proposed trivial names derived from the provenance of the most typical samples such as the Wyoming, Tatatilla, Chambers, and Otay (Cheto) types. Other names reveal (a-)typical properties like miscellaneous or ‘non-ideal’ montmorillonite. Differences in layer charge, tetrahedral substitution, high-temperature transformation, and Fe content were examined. A problem of the current classification systems is that several montmorillonites could not be assigned to the proposed types. The trivial

\* E-mail address of corresponding author: felih@gmx.de

\ddagger Present address: Bergstraße 47, 58300 Wetter (Ruhr), Germany

\dagger Deceased

DOI: 10.1346/CCMN.2009.0570111

names do not reflect some important chemical and structural parameters.

A new method which would allow modification and extension of the existing classification systems is proposed. Intercalation with alkylammonium ions, according to Lagaly and Weiss (1971), gives an insight into the charge distribution of 2:1 clay minerals. Because determining the layer charge of smectites is still a difficult and time-consuming task, various attempts were made to measure layer charge using quicker methods (Olis *et al.*, 1990; Christidis and Eberl, 2003). However, the alkylammonium method is still the best for a precise determination of the layer charge and charge distribution. Nevertheless, even today the average layer charge is mostly derived from the chemical formula calculated from the chemical analysis. The structural formula should be calculated according to the recommendation of Köster (1977), *i.e.* on the basis of the measured layer charge. Most of the formulae of smectites reported in the literature were based exclusively on the analytical composition leading to an overestimation of the permanent layer charge.

Brigatti (1983) established a relationship between the Fe content and the dehydroxylation temperature ( $T_{\text{DHX}}$ ). Tshipursky and Drits (1984) and Drits *et al.* (1995) discovered that the thermal behavior of dioctahedral 2:1 clay minerals is directly related to the structure of the octahedral sheet. Wolters and Emmerich (2007) presented a method to determine the *cis*- and *trans*-vacant sites based on Drits *et al.* (1998). Determination of the *cis/trans*-vacancies was the missing link for the comprehensive characterization of smectites (Emmerich *et al.*, 2009).

In this study, characterization of the smectites is focused on the following parameters: the layer charge determined by the alkylammonium method, the number of *cis*- and *trans*-vacancies of the octahedral sheets derived from simultaneous thermal analysis (STA), the total Fe content obtained by X-ray fluorescence (XRF), and the location of charges (tetrahedral/octahedral charges) derived from the stoichiometric composition of the mineral.

## MATERIALS AND METHODS

### *Materials and sample pre-treatment*

Twenty-eight smectite samples from various locations and of different origins were selected (Table 1). X-ray diffraction (XRD) analysis revealed that the samples contained minerals of the smectite group.

Depending on the amount of sample available, 10–100 g of each sample was subjected to chemical pre-treatment and size separation in order to enrich the smectites.

The samples were purified as described by Tributh and Lagaly (1986a, 1986b), Mehra and Jackson (1960), Dohrmann (1999), Emmerich (2000), and Carrado *et al.*

(2006). Because of the importance of the pretreatment reactions, they are reported here in detail:

(1) The carbonates were decomposed by an acetate buffer consisting of 2 M sodium acetate solution mixed with 2 M acetic acid in a 2:1 volume ratio and at pH = 4.8. Samples of 20 g were dispersed in 200 mL of the buffer solution without heating.

(2) Iron and Al (oxyhydr)oxides were dissolved by buffered dithionite-citrate solution. A 0.3 M sodium citrate solution was mixed with a 1 M sodium bicarbonate solution in an 8:1 ratio. The samples of ~20 g were dispersed in 225 mL of this solution, heated to 80°C, and then 5 g of solid dithionite was added. After 15 min at 80°C, the dispersion was cooled, centrifuged, and washed with sodium chloride solution before repeating the procedure. After washing with sodium chloride solution, organic matter was decomposed by careful and stepwise addition of hydrogen peroxide. For example, to a 900 mL sample suspension, 200 mL of a commercial 30% hydrogen peroxide solution was added, according to the general mixing rule used to adjust a 5% solution. When the first strong reaction decreased, a further 300 mL was added to obtain a 10% solution. Samples, which did not show a significant reaction, were heated to 60°C for 15 min to accelerate the reaction. Finally, the samples were washed four times with a 1 M NaCl solution, then with deionized water, until the remaining material was dispersed. All samples were treated in the same way, even if no substances which might affect the identification were present.

For fractionation, the dispersions of the purified bentonites were passed through a 63  $\mu\text{m}$  sieve. To avoid mutual influence of the settling particles, 2–2.5 g of the purified samples was dispersed per liter of deionized water. Because the untreated material of some of the samples amounted to 80 g or more, up to 40 L of deionized water was used for fractionation. The <2  $\mu\text{m}$  fraction of the purified samples was obtained by gravitational sedimentation; the <0.2  $\mu\text{m}$  fraction, by centrifugal sedimentation of the <2  $\mu\text{m}$  dispersions (in a constant-temperature centrifuge at 22°C) (Tributh and Lagaly, 1986b). The dispersions with <2  $\mu\text{m}$  and <0.2  $\mu\text{m}$  were coagulated with NaCl (the amount of NaCl depended on the amount of sample). The NaCl-containing dispersions were dialyzed until the conductivity of water reached 3  $\mu\text{S}/\text{cm}$ . The chloride-free fractions were dried at 65°C and milled slightly in an agate mortar.

The <2  $\mu\text{m}$  and <0.2  $\mu\text{m}$  fractions were characterized by XRD, layer charge, CEC, XRF, STA measurements, and Mössbauer spectroscopy. In most cases, the stoichiometric composition was calculated from the data from the <0.2  $\mu\text{m}$  fraction which commonly contains almost pure smectite whereas the <2  $\mu\text{m}$  fraction can contain free silica (quartz or cristobalite), mica/illite, or kaolinite. Where cristobalite was present in the <0.2  $\mu\text{m}$  fraction, it was quantified in order to correct the chemical analysis.

Table 1. The materials investigated, their provenance, and their suppliers.

Sample no	Name	Provenance	Supplier
2LP	Lago Pelegrino	Argentina	K. Emmerich/Forschungs- zentrum Karlsruhe (FZK)
3, 7th Mayo	7th Mayo	Argentina	K. Emmerich/FZK
4Jup	Jupiter	Argentina	K. Emmerich/FZK
5MC	Ca-montmorillonite	Italy, Mandas Cagliari	M.F. Brigatti/ University of Modena (UM)
6GPC	Ca-montmorillonite	Italy, S. Giuliano di Puglio, Campobasso	M.F. Brigatti/UM
7EMC	Ca-montmorillonite	Italy, S. Erocadi, Magliano, Campobasso	M.F. Brigatti/UM
8UAS	Ca-montmorillonite	Italy, Uri Alghero, Sassari	M.F. Brigatti/UM
10MBV	Fe-rich montmorillonite	Italy, Monte Brosimo, Vicenza	M.F. Brigatti/UM
12TR01	TR 01		R. Ahlers/Süd-Chemie (SC)
13TR02	TR 02		R. Ahlers/SC
14TR03	TR 03		R. Ahlers/SC
15TR04	TR 04		R. Ahlers/SC
16GR01	GR 01		R. Ahlers/SC
17GR02	GR 02		R. Ahlers/SC
18USA01	USA 01		R. Ahlers/SC
19USA02	USA 02		R. Ahlers/SC
20MEX01	MEX 01		R. Ahlers/SC
21D01	D 01		R. Ahlers/SC
24Beid	Beidellite	Germany, Unterruprath	G. Kahr/ETHZ
25Volclay	Volclay/ETH	USA, Wyoming	G. Kahr/ETHZ
26/27Valdol	Valdol, Bentonite C14	Italy, Valdagno	G. Kahr/ETHZ
28SB	SW B3 SB; Almeria	Spain, Almeria	K. Emmerich/FZK
31BAR 3		Armenia	R. Nüesch/FZK
32Volclay	SW B2 Vo, Volclay	USA	K. Emmerich/FZK
33CA	SW B1 CA, Calcigel	Germany	K. Emmerich/FZK
36M650	Mlety 650 (D)	Czech Republic	G. Kahr/ETHZ
37BB	Berkbond	UK, England	G. Kahr/ETHZ
38MW	Mill white n.4	USA, Arkansas	G. Kahr/ETHZ
39G Q-I	Geko Q-I	Italy	G. Kahr/ETHZ
41ValC18	Valdol, Bentonite C18	Italy, Valdagno	G. Kahr/ETHZ
42Linden	Linden	Germany, Bavaria	K. Emmerich/FZK

### XRD

X-ray diffraction of the powdered bulk materials and the fractions was used to identify the mineral impurities, and to confirm the absence of mixed-layer illite-smectite minerals. The cristobalite content in the  $<0.2 \mu\text{m}$  fraction was determined by comparing with an external standard.

Oriented samples were prepared by dispersing 80 mg of the  $<2 \mu\text{m}$  and  $<0.2 \mu\text{m}$  fractions in 2 mL of deionized water. The dispersions were placed, by means of a pipette, onto glass slides with a diameter of 2.5 cm and dried under atmospheric conditions overnight at room temperature. These samples were solvated for a minimum of 2 days with ethylene glycol in a desiccator under vacuum.

The XRD measurements were carried out using a Siemens D5000 device equipped with a graphite diffracted-beam monochromator ( $\text{CuK}\alpha$  40 kV, 40 mA,  $2-35(65)^\circ 2\theta$  with a step size of  $0.02^\circ 2\theta$  and 3 s/step, divergence and antiscattering slits of 0.6 mm, receiving slits of 0.1 and 1.0 mm).

As the smectite data for the Rietveld analysis (Ufer *et al.*, 2004) was not available at that time, the amount of cristobalite was determined by the external standard method. A silica gel showing the maximum broadened reflection at  $4.05 \text{ \AA}$ , *i.e.* at the same position as the sharp reflection of cristobalite in the sample, was selected as the external standard. A calibration curve was made from mixtures of the silica gel and a smectite (sample 18USA01) free of cristobalite. The net peak areas of the recorded samples and the external standards were determined with the *DiffracPlus* evaluation 10.0 (provided by Bruker). The absolute error of the method was 0.25 to 0.5% for a sample with 0–2% cristobalite and decreased with increasing amount of cristobalite. The samples were recorded at  $20.5-23.5^\circ 2\theta$  with a step size of  $0.02^\circ 2\theta$  and 20 s/step, divergence and antiscattering slits of 0.6 mm, and receiving slits of 0.1 and 1.0 mm.

### Layer charge

The layer-charge distribution of the smectites was determined by the alkylammonium method (Lagaly,

1981, 1989, 1994; Lagaly and Weiss, 1971). The interlayer cations of the smectites were displaced by alkylammonium ions of various chain lengths. The basal spacings of the alkylammonium derivatives were measured by XRD after washing with ethanol and drying (Lagaly, 1994).

To calculate the cation densities, the peak migration curve (according to Lagaly, 1981) was used. The mean layer charge was calculated from the cation densities and their relative frequencies.

Samples of 50 mg were dispersed in 3 mL n-alkylammonium formate solutions (with  $n_c = 4$  to 18 carbon atoms in the alkyl chain, except  $n_c = 17$ ). Alkylammonium formate solutions were chosen due to the greater solubility of the longer alkylammonium salts (G. Kahr, pers. comm., 2003). The dispersions were held at 65°C. After 24 h the solid was separated by centrifugation, washed with ethanol, and once again dispersed in fresh alkylammonium formate solution and stored again at 65°C. The samples were washed free of the excess alkylammonium formate with absolute ethanol (eight times for chain length  $n_c = 4$ –13, 13 times for chains  $n_c = 13$ –18). Two washings followed with reagent-grade ethanol. Textured samples were dried at 65°C and stored in a desiccator over  $P_2O_5$  until their basal reflections were recorded by XRD (Rühlicke and Kohler, 1981).

To estimate the mean layer charge ( $\xi_M$ ) from the basal spacing of one alkylammonium derivative ( $n_c = 12$  or 18), as recommended by Olis *et al.* (1990), the  $\xi_M$  determined by the series of alkylammonium ions was related to the basal spacing of the dodecylammonium derivative. By a regression model the resulting relationship  $d_{001\ n_c=12} = 5.52 + 32.98 * \xi_M$  was used.

### CEC

To determine the CEC, the exchangeable cations were replaced by Cu triethylenetetramine cations (Meier and Kahr, 1999; Ammann *et al.*, 2005). Prior to this exchange the samples were stored over magnesium nitrate (53% r.h.) for at least 24 h. 50 mg of the samples was dispersed in 6 mL of a 0.01 M Cu-complex solution. 10 mL of deionized water was added and the dispersions were shaken for 2 h. The solution was centrifuged at 3500 rpm for 10 min. The CEC was related to the dry weight of the completely dehydrated montmorillonite at 350°C; the solid content of the air-dried samples was determined by thermogravimetry. The depletion of the Cu-triethylenetetramine cations in solution was determined by photometry at 580 nm.

### XRF

The weight loss of the <0.2  $\mu\text{m}$  fractions (milled to <40  $\mu\text{m}$ ) was determined by heating 1000 mg (in a few cases 600 mg) for 10 min at 1030°C. After mixing the residue with 5 g of lithium metaborate (for 600 mg samples 2.5 g lithium metaborate and 2.415 g lithium tetraborate) and 25 g lithium bromide, the material was

fluxed in Pt/Au crucibles in an automatic melting furnace for 20 min at 1200°C. Measurements were performed with the wavelength dispersive X-ray spectrometers (WD-XRF) PW 1480 and PW 2400 controlled by the Philips X40 software. The PW 1480 with a 2.5 kW/80kV chromium anode X-ray tube was used for the elements Ca, K, Ti, Ba, Sc, Cs, and Sb. The PW 2400 with a 2.7 kW/60 kV rhodium anode X-ray tube was used for Si, Al, Fe, Mn, Mg, Na, P, S, F, Cl, As, Bi, Ce, Cr, Cu, Ga, Hf, La, Mo, Nb, Nd, and Ni.

### Structural formula

Ensuring that the chemical analysis represents only the mineral of interest is essential. To accomplish this, the XRF data from cristobalite-containing samples were corrected using the calibrations obtained by the external standard method. Different assumptions have been made in the literature regarding corrections for  $TiO_2$  and  $P_2O_5$ . Van Olphen (1963) and Köster (1977) considered  $TiO_2$  and  $P_2O_5$  as mineral impurities. Bain and Smith (1992) suggested that any Ti present in the analysis of clays probably occurs as anatase. In the absence of direct evidence of a particular Ti mineral, the quantity of  $TiO_2$  was simply subtracted. Bain and Smith (1992) assumed that small amounts of phosphates and sulfates were present as unidentified impurities. Newman (1987) assigned  $TiO_2$  to the octahedral sheet of clay minerals. In the present study,  $TiO_2$  or Ti in the clay mineral structure was not considered.

The stoichiometric elemental composition of the smectites was calculated using two different methods. The first (Stevens, 1945) was based on the assumption of 22 negative charges per formula unit (Table 2). In the second method, the measured layer charge was involved in the calculation of the structural formula as recommended by Köster (1977) (Table 3). The layer charge derived from the structural formula according to Stevens (1945) was distinctly different from the measured layer charge. Nevertheless, both methods were applied for comparison as most characterizations of smectites reported in the literature refer to the calculated and not to the measured layer charge. The method of Stevens (1945) is quite common but the calculation procedure of Köster (1977) should be given priority because, in this method, 22 cationic charges are distributed into tetrahedral, octahedral, and interlayer positions while considering the measured layer charge.

The CEC values are unhelpful for smectites, as up to 20% of the CEC is pH-dependent (Lagaly, 1981; Bergaya *et al.*, 2006).

Köster (1977) used relative cation numbers and relative cation charges (referred to as 'rKZ' and 'rKL' in the original work). The weight percents from the chemical analyses were transformed into rKZ and rKL values. The rKL values correspond to the 'equivalents' of cations used by Bain and Smith (1992). The Bain and Smith (1992) or Stevens (1945) proportionality factor is

Table 2. Calculation of the structural formula of montmorillonite according to Stevens (1945), sample 41 Val C18.

Cation oxide	Corrected oxide mass (%) O	Molar weight (g/mol) M	Cation charge* number in oxide F	Cation charge C	Equivalent	Equivalent''	Cation	Atomic ratio E''/C
					E = (O*F)/M	E'' = (22/ΣE)*E		
SiO <sub>2</sub>	55.88	60.07	4	4	3.721	15.327	<sup>IV</sup> Si <sup>4+</sup> <sup>IV</sup> Al <sup>3+</sup>	3.83 <sup>#</sup> 0.17 <sup>#</sup> 4.00
Al <sub>2</sub> O <sub>3</sub>	17.07	101.96	6	3	1.004	4.136	<sup>VI</sup> Al <sup>3+</sup>	1.21 <sup>#</sup>
Fe <sub>2</sub> O <sub>3</sub>	8.71	159.67	6	3	0.327	1.349	<sup>VI</sup> Fe <sup>3+</sup>	0.45
FeO	0.00	71.85	2	2	0.000	0.000	<sup>VI</sup> Fe <sup>2+</sup>	0.00
TiO <sub>2</sub>	0.00	79.88	4	4	0.000	0.000	<sup>VI</sup> Ti <sup>4+</sup>	0.00
MgO	3.58	40.31	2	2	0.177	0.731	<sup>VI</sup> Mg <sup>2+</sup>	0.37
Mn <sub>2</sub> O <sub>3</sub>	0.00	157.88	6	3	0.000	0.000	<sup>VI</sup> Mn <sup>3+</sup>	0.00
MnO	0.01	70.94	2	2	0.000	0.001	<sup>VI</sup> Mn <sup>2+</sup>	0.00 2.03
CaO	0.15	56.08	2	2	0.005	0.022	Ca <sup>2+</sup>	0.01
Na <sub>2</sub> O	2.53	61.97	2	1	0.082	0.336	Na <sup>+</sup>	0.34
K <sub>2</sub> O	1.12	94.2	2	1	0.024	0.098	K <sup>+</sup>	0.10

<sup>#</sup> all Si<sup>4+</sup> are assigned to tetrahedral sites, the remaining sites are filled with Al<sup>3+</sup>, the remaining Al<sup>3+</sup> are assigned to octahedral sites.

equivalent to Köster's factor  $X = \Sigma r_{KL}/(22-\xi)$ . In contrast to Köster (1977), Stevens (1945) refers only to 22 anionic charges instead of 22 anionic charges minus the measured layer charge (Tables 2, 3). Calculating  $r_{KZ}/r_{KL}$  gives the number of cations per f.u.

In summary, the data necessary to obtain the structural formulae of smectites are chemical composition (e.g. from XRF), the measured layer charge, and the CEC for crosschecking purposes.

#### Location of charge

The location of charge due to substitutions in the octahedral and tetrahedral sheets was derived from the stoichiometric composition according to Köster (1977).

#### Simultaneous thermal analysis (STA)

The STA measurements were performed using an STA 449 C Jupiter from NETZSCH-Gerätebau GmbH with a thermogravimetry/differential scanning calorimetry (TG/DSC) sample holder. The STA was connected to a quadrupole mass spectrometer 403 C Aëolos from IPI/InProcess Instruments/NETZSCH-Gerätebau GmbH. All samples were allowed to equilibrate at a r.h. of 53% in a desiccator above saturated Mg(NO<sub>3</sub>)<sub>2</sub> solution for at least 48 h. The conditions for the STA measurements are reported in Table 4.

*PeakFit* (Jandel Scientific Software) was used for peak deconvolution of the mass spectrometer curves of evolved water (m/e = 18) during dehydroxylation (300–900°C). This method allowed the determination of the *cis/trans* vacancies of the samples (Wolters and Emmerich, 2007).

Drits *et al.* (1995) discriminated between *trans*-vacant and *cis*-vacant sites by the maximum of the

dehydroxylation peaks below (for *tv* sites) and above 600°C (for *cv* sites). Wolters and Emmerich (2007) bolstered confidence in this assumption by finding it to also be true under other experimental conditions. To determine the number of *tv* and *cv* octahedral sheets, the relative area of all peaks with maxima below 600°C and above 600°C were summed.

#### Mössbauer spectroscopy

Mössbauer spectra of the bulk material and of the <0.2 μm fraction of 10 samples were taken at 298 K and at 4.2 K using a <sup>57</sup>Co source to identify the presence of Fe oxides in the bulk material. Insufficient removal of Fe oxides or oxidation of Fe(II) in the smectite structure was also investigated. The purpose was to check the reliability of the structural formula derived from chemical analyses according to Köster (1977), in particular the Fe(III)/Fe(II) ratio. In addition, isomer shift (IS) and quadrupole splitting (QS) were determined for four low-charged *cv* and *tv* (ferrian) beidellitic montmorillonites. For experimental details see Wagner and Kyek (2004).

## RESULTS AND DISCUSSION

#### Identification of smectites

The XRD patterns of most textured, air-dried, Na<sup>+</sup>-saturated samples showed  $d_{001} = 11.3\text{--}12.6$  Å depending on the laboratory atmosphere (35–60% r.h.). All samples expanded with ethylene glycol from  $d_{001} = 16.8$  to 17.1 Å indicating smectites (Table 5). Most samples displayed rational series of basal reflections; an example is given for sample 4 JUP (Figure 1).

When the XRD patterns revealed a very small shoulder at ~10 Å, the presence of mixed-layer minerals was tested

Table 3. Calculation of the structural formula of montmorillonite according to Köster (1977), sample 41 Val C18: relative cation numbers and charges for octahedral and tetrahedral cations and interlayer cations refer to the measured layer charge.

Cation oxide	Corrected oxide mass (%) O	Molar weight (g/mol) M	Number in oxide N	Cation charge C	Relative cation number $rKZ = (O \cdot N \cdot 1000) / M$	Relative cation charge $rKL = rKZ \cdot C$	rKL/X	rKZ/X	Cation	Atomic ratio
SiO <sub>2</sub>	55.88	60.07	1	4	930	3720	15.43	3.86	IV Si <sup>4+</sup> IV Al <sup>3+</sup>	3.86 <sup>#</sup> 0.14 <sup>#</sup> 4.00
Al <sub>2</sub> O <sub>3</sub>	17.07	101.96	2	3	335	1005	4.16	1.39	V <sup>I</sup> Al <sup>3+</sup>	1.25 <sup>#</sup>
Fe <sub>2</sub> O <sub>3</sub>	8.71	159.67	2	3	109	327	1.36	0.45	V <sup>I</sup> Fe <sup>3+</sup>	0.45
FeO	0.00	71.85	1	2	0	0	0.00	0.00	V <sup>I</sup> Fe <sup>2+</sup>	0.00
TiO <sub>2</sub>	0.00	79.88	1	4	0	0	0.00	0.00	V <sup>I</sup> Ti <sup>4+</sup>	0.00
MgO	3.58	40.31	1	2	89	178	0.74	0.37	V <sup>I</sup> Mg <sup>2+</sup>	0.37
Mn <sub>2</sub> O <sub>3</sub>	0.00	157.88	2	3	0	0	0.00	0.00	V <sup>I</sup> Mn <sup>3+</sup>	0.00
MnO	0.01	70.94	1	2	0	0	0.00	0.00	V <sup>I</sup> Mn <sup>2+</sup>	0.00
Interlayer cation										Interlayer cation = ( $\xi \cdot R / 100$ ) / C
CaO	0.15	56.08	3.98	2					Ca <sup>2+</sup>	0.01
Na <sub>2</sub> O	2.53	61.97	66.58	1					Na <sup>+</sup>	0.20
K <sub>2</sub> O	1.12	94.2	29.44	1					K <sup>+</sup>	0.09

Calculation of X:  $X = rKL \cdot (22 - \xi_{O}) = 241.16$  with  $\Sigma rKL = 5231$  and  $\xi_{M} = 0.31$  eq/f.u.  
<sup>#</sup>all Si<sup>4+</sup> are assigned to tetrahedral sites, the remaining sites are filled with Al<sup>3+</sup>, the remaining Al<sup>3+</sup> are assigned to octahedral sites

Table 4. STA conditions.

	TG/DSC/MS
Amount of sample	100 mg
Grain size	powder
Packing density	loosely packed, no pressing
Reference material	empty crucible with lid
Furnace atmosphere	50 mL/min air + 20 mL/min N <sub>2</sub>
Crucibles	Pt/Rh with lid
Thermocouples	Pt/Pt <sub>90</sub> Rh <sub>10</sub>
Heating rate	10 K/min
Temperature range	35–1000°C

by saturating the sample with SrCl<sub>2</sub> and air-drying. This treatment shifted the first basal spacing to 15.4 Å, typical of smectites with divalent interlayer cations. The simultaneous disappearance of the reflection at ~10 Å was the confirming test that mixed-layer minerals were absent and the sample was a pure smectite.

#### Layer charge and CEC

The mean layer charge of the smectites ranged from 0.27 to 0.38 eq/f.u. Mean layer charge determined according to Lagaly (1994) and estimated using the

method of Olis *et al.* (1990) differed by <0.02 eq/f.u. (Table 6).

Three different histograms for charge distribution were observed. Bimodal distributions were dominant and monomodal distributions were rare. The distribution of some smectites showed three maxima. In most cases bimodal distributions showed a maximum at lower charge densities or two maxima of similar height (Figure 2a,b). Samples 7EMC, 12TR01, and 19USA02 showed equivalent weighted frequencies.

Samples 6GPC, 28SB, 33CA, and 36M650 revealed monomodal distributions (Figure 3a). Three clear maxima were found for 14TR03, 38MW, and 41ValC18 (Figure 3b).

#### CEC

The bulk material had the smallest CEC value, corresponding to the smectite contents in the samples. In most cases, CEC increased with decreasing particle size of the fractions (Table 5) due to enrichment of smectite. However, a few <0.2 µm fractions had smaller CEC values than the <2 µm fraction. Similar behavior was reported in other studies (*e.g.* Kaufhold *et al.*, 2002). Jasmund and Lagaly (1993) documented the different charge densities of various particle-size fractions of

Table 5. *d* values (Å) of basal reflections of the <0.2 µm fractions.

Sample no.	Air-dried, Na <sup>+</sup> -saturated			EG-saturated				
	<i>d</i> <sub>001</sub>	<i>d</i> <sub>002</sub>	<i>d</i> <sub>004</sub>	<i>d</i> <sub>001</sub>	<i>d</i> <sub>002</sub>	<i>d</i> <sub>003</sub>	<i>d</i> <sub>004</sub>	<i>d</i> <sub>005</sub>
2LP	11.8	n.d.	3.1	17.1	8.5	5.7	4.3	3.4
3, 7th Mayo	12.4	n.d.	3.2	16.6	8.5	n.d.	n.d.	n.d.
4JUP	12.4	n.d.	3.1	17.0	8.6	5.6	4.3	3.4
5MC	11.4	n.d.	3.1	16.9	8.6	5.7	n.d.	n.d.
6GPC	11.7	n.d.	3.1	16.8	8.6	5.6	n.d.	n.d.
7EMC	11.1	n.d.	3.1	17.1	8.5	5.7	n.d.	3.2
8UAS	11.9	n.d.	3.1	16.7	8.5	5.6	n.d.	3.1
12TR01	11.5	n.d.	3.2	16.8	8.5	5.6	n.d.	n.d.
13TR02	12.4	6.2	3.1	16.7	8.5		n.d.	n.d.
14TR03	11.9	n.d.	3.2	16.6	8.5	5.6	n.d.	n.d.
16GR01	12.3	6.2	3.1	16.9	8.5		n.d.	n.d.
17GR02	12.4	6.2	3.1	17.0	8.5	5.7	n.d.	n.d.
18USA01	11.9	n.d.	3.1	16.8	8.5	5.6	n.d.	n.d.
19USA02	12.2	6.1	3.1	16.6	8.4	5.6	n.d.	n.d.
21D01	12.4	n.d.	3.1	17.0	8.5	5.6	4.3	3.4
24Beid*	12.5	6.2	3.1	16.2	8.5	5.6	n.d.	3.4
25 Volclay*	12.6	6.2	3.1	17.0	8.5	5.7	4.3	3.4
26-27 Valdol C14*	12.6	6.2	3.1	16.8	8.6	5.6	4.3	3.4
28SB	12.8	6.2	3.1	17.0	8.6	5.6	n.d.	3.4
31BAR3	12.7	n.d.	3.1	17.1	8.6	5.6	4.3	3.4
32Volclay	12.5	n.d.	3.1	17.3	8.6	5.7	4.3	3.4
33CA	12.8	n.d.	3.1	17.2	8.7	5.7	4.3	3.4
36M650	12.6	n.d.	3.1	17.1	8.6	5.6	n.d.	3.4
37BB	12.4	n.d.	3.1	17.1	8.6	5.6	n.d.	3.4
38MW	13.1	n.d.	3.1	17.1	8.6	5.7	n.d.	3.4
39G Q-I	12.8	n.d.	3.1	16.9	8.6	5.6	4.3	3.4
41Val C18	12.5	n.d.	3.1	17.0	8.6	5.7	n.d.	3.4
42Linden*	12.8	6.2	3.1	17.3	8.6	5.7	n.d.	3.4

n. d.: reflection was too weak to detect

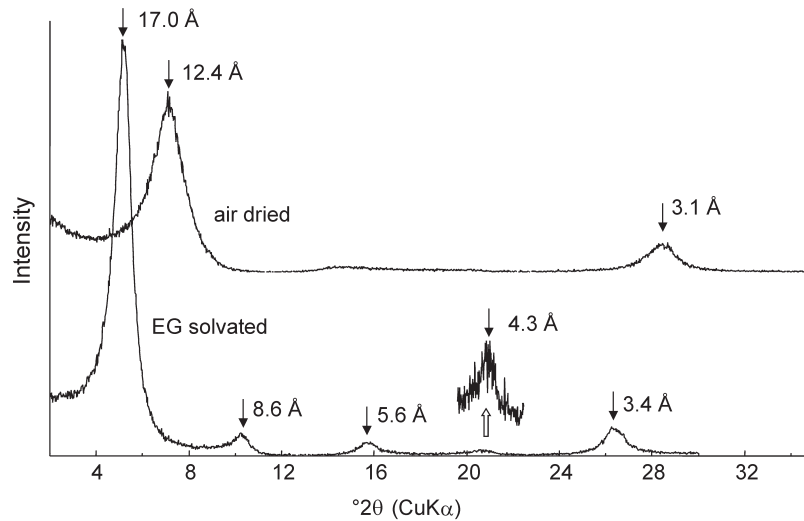


Figure 1. An example of the rational series of basal reflections, presented for sample 4 JUP.

Table 6. CEC, layer charge, and location of charge.

Sample no.	CEC (meq/100 g)			Layer charge (eq/f.u.) of <0.2 μm				Tetrahedral charge (%)
	Bulk	<2 μm	<0.2 μm	Measured <sup>1</sup>	Measured <sup>2</sup>	Calculated <sup>3</sup>	Calculated <sup>4</sup>	
2LP	91	96	94	0.28	0.29	0.29	0.37	24
3, 7th Mayo	77	89	89	0.3	0.31	0.31	0.42	29
4JUP	70	81	91	0.29	0.30	0.26	0.37	62
5MC	69	85	81	0.28	0.28	0.32	0.40	13
6GPC	48	58	75	0.33	0.34	0.34	0.45	38
7EMC	62	69	73	0.28	0.29	0.29	0.40	38
8UAS	81	101	97	0.34	0.33	0.37	0.48	3
12TR01	79	91	99	0.36	0.38	0.35	0.42	17
13TR02	103	112	113	0.35	0.37	0.35	0.48	6
14TR03	119	122	112	0.37	0.38	0.36	0.47	3
16GR01	95	102	101	0.31	0.31	0.32	0.40	9
17GR02	54	63	73	0.29	0.3	0.30	0.38	33
18USA01	84	91	93	0.27	0.28	0.26	0.41	15
19USA02	76	94	98	0.30	0.31	0.30	0.39	17
21D01	73	87	85	0.29	0.31	0.31	0.42	29
24Beid*	n.d.	101	n.d.	n.d.	0.38	0.39	0.54	77
25 Volclay*	n.d.	87	n.d.	n.d.	0.27	0.26	0.45	12
26-27 Valdol C14*	n.d.	83	n.d.	n.d.	0.27	0.27	0.55	37
28SB	75	95	102	0.36	0.39	0.36	0.47	19
31BAR3	77	87	97	0.32	0.32	0.30	0.41	3
32Volclay	85	88	81	0.27	0.27	0.28	0.39	11
33CA	63	75	87	0.30	0.30	0.31	0.42	45
36M650	71	87	77	0.3	0.30	0.27	0.34	70
37BB	78	90	89	0.28	0.26	0.25	0.42	48
38MW	89	86	84	0.27	0.26	0.26	0.37	50
39G Q-I	95	108	109	0.35	0.37	0.39	0.41	15
41Val C18	54	84	85	0.31	0.37	0.30	0.45	47
42Linden*	n.d.	103	n.d.	0.32	n.d.	0.35	0.36	14

<sup>1</sup> Lagaly (1994)<sup>2</sup> Olis *et al.* (1990)<sup>3</sup> Köster (1977)<sup>4</sup> Stevens (1945)

\* &lt;2 μm fraction

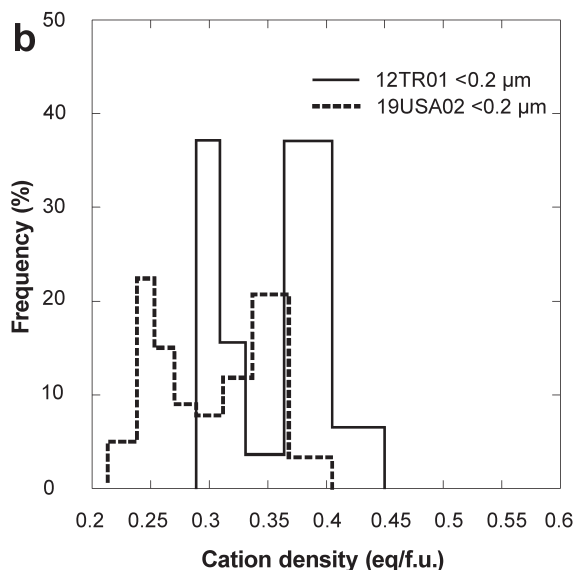
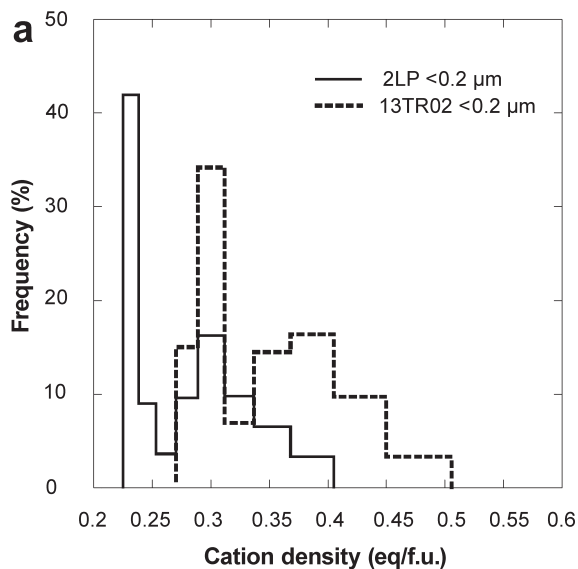


Figure 2. Example of bimodal charge distributions with: (a) the maximum at lower charge densities; and (b) with two similar maxima.

smectites. The  $<0.2 \mu\text{m}$  fraction of some samples probably consists of lower-charged layers compared to the  $<2 \mu\text{m}$  fraction, also reported by Grim and Kulbicki (1961).

#### Analytical composition and structural formulae calculation

The chemical composition of the  $<0.2 \mu\text{m}$  fractions (Table 7) is reported without correction of the  $\text{SiO}_2$  content due to free cristobalite. Seven samples contained cristobalite: 5EMC contained 1%  $\text{SiO}_2$ ; 7EMC, 19%; 8UAS, 9%; 12TR01, 13%; 14TR03, 1%; 17GR02, 21%; and 31BAR3, 1%. The structural formulae were calculated considering these cristobalite contents.

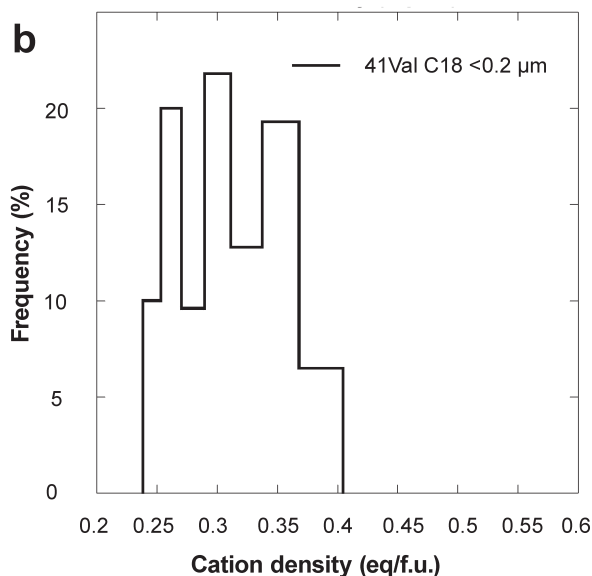
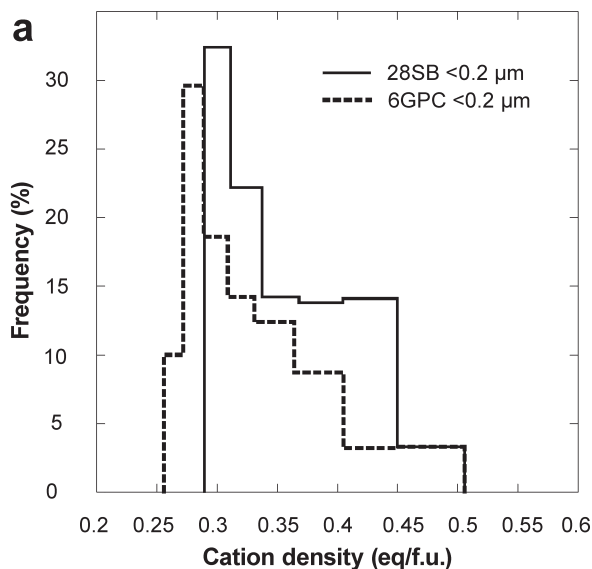


Figure 3. Example of (a) monomodal charge distribution and (b) 'trimodal' charge distributions.

Homo-ionic saturation with  $\text{Na}^+$  ions was successful as none of the treated samples contained  $\text{Ca}^{2+}$  as the interlayer cation – the XRF analyses revealed CaO values of  $<0.05\%$ . The amount of  $\text{K}^+$  ions in the interlayer space was  $<0.1 \text{ mol/f.u.}$ , except for 6GPC which had  $0.11 \text{ mol K}^+/\text{f.u.}$

On average, the Na-saturated smectites had, including interlayer cations, a molar mass of 376 (Table 8). All smectites of the montmorillonite–beidellite series showed substitution in the tetrahedral and the octahedral sheets. Samples 5MC, 8UAS, 13TR02, 14TR03, 16GR01, 18USA01, 25Volclay, 31BAR3, and 32Volclay contained  $<0.05 \text{ mol/f.u.}$  of tetrahedral  $\text{Al}^{3+}$ . The proportion of tetrahedral charge of these samples

Table 7. Chemical composition (wt.%) of the <0.2  $\mu\text{m}$  fraction, as obtained by XRF analyses.

Sample no.	SiO <sub>2</sub>	TiO <sub>2</sub>	Al <sub>2</sub> O <sub>3</sub>	Fe <sub>2</sub> O <sub>3</sub>	MnO	MgO	CaO	Na <sub>2</sub> O	K <sub>2</sub> O	P <sub>2</sub> O <sub>5</sub>	SO <sub>3</sub>	Cl	F	LOI	$\Sigma$ XRF
2LP	58.97	0.14	20.31	4.45	0.01	2.84	0.04	2.81	0.05	0.01	0.01	0.01	0.12	10.03	99.78
3, 7th Mayo	57.84	0.70	18.31	6.91	0.05	3.08	0.01	2.76	0.42	0.02	0.01	0.00	0.07	9.55	99.69
4JUP	56.00	0.75	19.89	7.52	0.02	1.86	0.05	2.70	0.28	0.02	0.01	0.01	0.14	10.50	99.73
5MC	59.36*	0.41	17.56	6.36	0.01	3.40	0.01	2.90	0.12	0.02	0.03	0.03	0.10	9.45	99.73
6GPC	56.62	0.38	19.00	6.00	0.01	3.29	0.04	2.62	1.41	0.07	0.01	0.00	0.09	10.13	99.64
7EMC	66.80*	0.11	17.57	2.61	0.00	2.48	0.01	2.70	0.05	0.01	<0.01	0.00	<0.05	7.41	99.72
8UAS	63.59*	0.15	16.49	3.10	0.03	4.16	0.01	3.31	0.07	0.01	<0.01	0.00	<0.05	8.83	99.73
12TR01	61.31*	0.07	16.83	1.11	0.01	3.35	0.01	2.76	0.07	0.00	<0.01	0.00	0.16	14.14	99.81
13TR02	57.27	0.20	16.79	3.24	0.01	5.16	0.01	3.43	0.10	0.02	0.01	0.00	0.05	13.49	99.73
14TR03	59.96*	0.08	17.96	1.73	0.01	5.59	0.01	3.67	0.03	0.01	0.01	0.00	<0.05	10.69	99.73
16GR01	60.46	0.13	20.87	1.74	0.01	3.56	0.01	3.16	0.05	0.00	<0.01	0.01	0.08	9.70	99.77
17GR02	67.63*	0.14	17.80	1.45	0.00	2.33	0.01	2.38	0.03	0.01	<0.01	<0.002	0.05	7.96	99.77
18USA01	58.82	0.16	19.51	4.11	0.02	3.13	<0.005	3.03	0.08	0.01	<0.01	<0.002	<0.05	10.89	99.75
19USA02	60.30	0.23	18.99	5.86	0.00	3.13	0.07	3.05	0.04	0.05	<0.01	<0.002	<0.05	8.00	99.71
21D01	58.27	0.18	18.67	6.16	0.02	3.42	<0.005	2.85	0.39	0.03	<0.01	<0.002	<0.05	9.71	99.70
24Beid**	52.58	0.03	25.37	0.13	0.01	2.31	0.03	4.12	0.03	0.01	<0.01	0.01	<0.05	15.15	99.76
25 Volclay**	56.97	0.13	19.78	3.41	0.00	2.21	0.05	3.26	0.08	0.01	0.05	0.01	0.10	13.75	99.77
26-27 Valdol C14**	53.05	1.16	16.12	7.43	0.01	3.15	0.07	2.83	1.49	0.02	0.03	0.02	0.06	14.23	99.63
28SB	58.62	0.15	18.03	4.55	0.02	4.73	0.03	3.08	0.60	0.01	<0.01	0.01	0.09	9.80	99.73
31BAR3	58.97*	0.31	16.83	5.56	0.01	3.70	0.04	2.73	0.47	0.01	0.01	0.01	0.19	11.03	99.78
32Volclay	61.81	0.15	21.41	3.78	0.00	2.32	0.03	2.99	0.10	0.03	<0.01	0.01	<0.05	7.07	99.67
33CA	58.01	0.28	20.20	5.85	0.02	3.19	0.05	2.67	0.96	0.02	<0.01	0.01	<0.05	8.40	99.65
36M650	53.03	3.45	17.78	8.47	0.02	2.70	0.08	2.16	0.25	0.17	<0.01	<0.002	0.06	11.18	99.32
37BB	56.06	0.40	16.07	11.16	0.00	2.69	0.01	2.98	0.11	0.03	<0.01	<0.002	<0.05	10.04	99.56
38MW	56.70	0.18	18.26	8.34	0.01	2.75	0.02	2.81	0.07	0.04	0.03	0.02	<0.05	10.49	99.70
39G Q-I	56.83	0.42	17.27	4.57	0.04	4.42	0.01	3.05	0.25	0.02	<0.01	0.01	0.09	12.78	99.75
41Val C18	55.47	0.28	16.94	8.65	0.01	3.55	0.15	2.51	1.11	0.10	<0.01	0.01	0.11	10.87	99.71
42Linden**	61.85	0.00	20.9	3.86	0.00	4.08	0.00	2.97	0.00	n.d.	n.d.	n.d.	n.d.	7.16	100.82

\* Presence of cristobalite: 5EMC 1%, 7EMC 19%, 8UAS 9%, 12TR01 13%, 14TR03 1%, 17GR02 21% and 31BAR3 1% .

\*\* <2  $\mu\text{m}$  fraction

n.d.: not determined

did not exceed 15% of the total charge. In the octahedral sheet, Mg mainly substituted for Al. When the Fe content exceeded 0.3 mol/f.u., Fe ions became the dominant substituting ions. Samples 3, 7th Mayo, 4JUP, 26Valdol C14, 33CA, 36M 650, 37BB, 38MW, and 41Valdol C18 showed a molar Fe/Mg ratio of 1.1–2.5 (Table 8).

All smectites analyzed displayed an octahedral filling between 2 and 2.07 mol/f.u. Vogt and Köster (1978) also observed slight oversaturation of the octahedral positions. The Mg ions are probably clustered in the octahedral sheet leading to the formation of trioctahedral domains. Brigatti (1983) showed that the octahedral occupancy of 2 mol/f.u. is incorrect regarding the  $b$  values derived from  $d_{060}$ . Greater  $b$  values are probably due to trioctahedral domains and favor occupancies >2 mol/f.u. in the octahedral sheet.

The chemical formulae of all samples were also calculated according to Stevens (1945). Theoretical layer charges derived from these formulae were distinctly different from the independently measured values with differences of up to 0.2 eq/f.u. (Figure 4). Octahedral cation populations calculated by the

Stevens method varied between 1.93 and 2.05 mol/f.u. but were mostly <2.0.

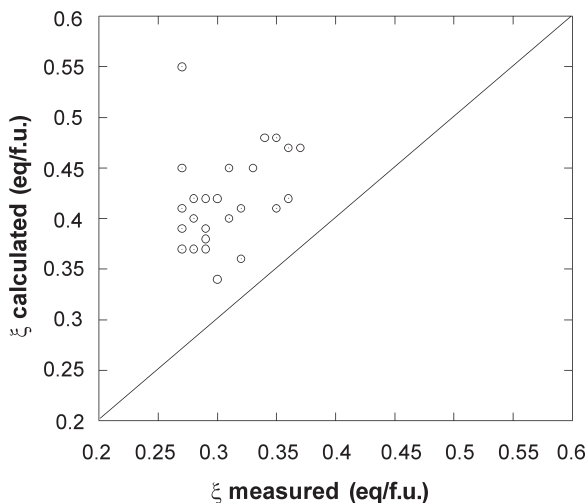


Figure 4. Layer charge determined by the alkylammonium method and the theoretical layer charge calculated from the stoichiometric composition according to Stevens (1945).

Table 8. Structural formulae based on  $O_{10}(OH)_2$  (Köster, 1977) given in mol/f.u. Total Fe content determined as  $Fe^{3+}$  (<0.2  $\mu m$  fraction).

Sample no	$IVSi^{4+}$	$IVAl^{3+}$	$VIAl^{3+}$	$VIFe^{3+}$	$VIMg^{2+}$	$\Sigma O^{**}$	$Ca^{2+}$	$Na^+$	$K^+$	Molar mass
2LP	3.93	0.07	1.52	0.22	0.28	2.02	0.00	0.28	0.01	373.21
3, 7th Mayo	3.91	0.09	1.37	0.35	0.31	2.03	0.00	0.27	0.04	378.08
4JUP	3.84	0.16	1.45	0.39	0.19	2.03	0.00	0.23	0.02	377.77
5MC	3.96	0.04	1.36	0.32	0.34	2.02	0.00	0.31	0.01	376.66
6GPC	3.87	0.13	1.40	0.31	0.33	2.04	0.00	0.22	0.12	379.07
7EMC	3.89	0.11	1.58	0.16	0.3	2.04	0.00	0.28	0.00	371.92
8UAS	3.99	0.01	1.41	0.17	0.45	2.03	0.00	0.36	0.01	373.49
12TR01	3.94	0.06	1.56	0.07	0.41	2.04	0.00	0.34	0.01	370.47
13TR02	3.98	0.02	1.36	0.17	0.54	2.07	0.00	0.34	0.01	373.86
14TR03	3.99	0.01	1.42	0.09	0.56	2.07	0.00	0.36	0.00	371.58
16GR01	3.97	0.03	1.58	0.09	0.35	2.02	0.00	0.31	0.00	369.62
17GR02	3.9	0.10	1.65	0.09	0.29	2.03	0.00	0.3	0.00	369.74
18USA01	3.96	0.04	1.51	0.21	0.31	2.03	0.00	0.25	0.01	372.46
19USA02	3.95	0.05	1.42	0.29	0.31	2.02	0.00	0.29	0.00	375.02
21D01	3.91	0.09	1.39	0.31	0.34	2.04	0.00	0.23	0.03	375.52
24Beid*	3.70	0.3	1.8	0.01	0.24	2.05	0.00	0.38	0.00	369.72
25 Volclay*	3.97	0.03	1.59	0.18	0.23	2.00	0.00	0.25	0.01	371.01
26-27 Valdol C14*	3.9	0.10	1.30	0.41	0.35	2.06	0.00	0.17	0.09	380.16
28SB	3.93	0.07	1.36	0.23	0.47	2.06	0.00	0.3.0	0.06	376.49
31BAR3	3.99	0.01	1.36	0.29	0.38	2.03	0.00	0.25	0.04	375.79
32Volclay	3.97	0.03	1.59	0.18	0.22	2.01	0.00	0.27	0.01	370.17
33CA	3.86	0.14	1.44	0.29	0.32	2.05	0.00	0.22	0.08	377.22
36M650	3.81	0.19	1.32	0.46	0.29	2.07	0.00	0.23	0.03	380.96
37BB	3.88	0.12	1.19	0.58	0.28	2.05	0.00	0.24	0.01	383.44
38MW	3.87	0.13	1.34	0.43	0.28	2.05	0.00	0.25	0.01	379.33
39GQ-I	3.94	0.06	1.35	0.24	0.45	2.04	0.00	0.36	0.03	376.51
41ValC18	3.86	0.14	1.25	0.45	0.37	2.07	0.01	0.20	0.09	382.57
42Linden*	3.95	0.05	1.46	0.18	0.39	2.03	0.00	0.35	0.00	373.28

\* <2  $\mu m$  fraction, \*\*  $\Sigma O$  = total octahedral cations

Unless otherwise stated, all diagrams in the present study refer to data calculated according to Köster (1977).

According to Mössbauer measurements of selected samples, 95–100% of the total Fe content in the octahedral sheet was  $Fe(III)$  (Wolters, 2005). Recalculation of the chemical formulae with the  $Fe(II)$  content led to maximum changes of  $\pm 0.02$  mol/f.u. Tetrahedrally coordinated  $Fe(III)$  was undetected. In general, correction of the stoichiometric composition for montmorillonites with small amounts of Fe was, therefore, unnecessary.

#### Location of charge

Twenty five samples of the smectites analyzed had a tetrahedral charge which was <50% of the total charge, *i.e.* 20 samples with 10–50% and five samples with <10% tetrahedral charge (8UAS, 13TR02, 14TR03, 16GR01, 31BAR) (Table 5). Only three samples (4Jup, 24Beid, 36M650) needed to be considered as montmorillonitic beidellite (Emmerich *et al.*, 2009).

#### Discrepancies between layer charge and CEC values

Layer charge determined solely from the chemical analysis is, on average, ~28% greater than that measured

directly by the alkylammonium method (Figure 4, Table 6).

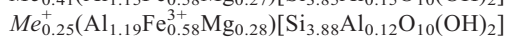
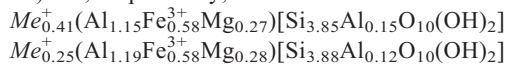
An extreme difference of 50% was found for sample 26/27ValdolC14. Similar differences were documented by Laird *et al.* (1989) who explained the difference by assuming an inaccurate estimate of the packing density of the alkylammonium ions in the interlayer space. However, the present CEC values are in agreement only with the measured layer charges.

Kaufhold *et al.* (2002) developed a method for quantifying the montmorillonite content in bentonites. The layer charge was calculated by a combination of different methods. The method requires determination of the CEC measured at pH 4, and the average molar mass obtained by XRF of the montmorillonite in question. Layer charge obtained in this way agrees with the measured values. This supports the accuracy of the alkylammonium method in spite of the assertion by Laird *et al.* (1989).

Comparison of calculated and measured layer charge supports the accuracy of the structural formula calculation of Köster (1977). The calculated CEC values differ from the measured CEC values for both of the structural-formula calculations. The CEC values derived from the

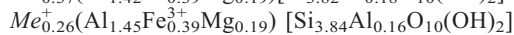
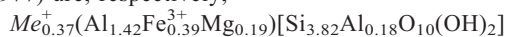
structural formula according to Stevens (1945) are generally greater than the measured CEC values. However, the calculated CEC values should be less than the measured values because ~10–20% of the charge is located at the edge of the smectite particles (Lagaly, 1981; Kaufhold *et al.*, 2002). The CEC values calculated according to Köster (1977) satisfy this condition (Figure 5) as illustrated by the following example.

The stoichiometric composition calculated for sample 37BB by the methods of Stevens (1945) and Köster (1977) are, respectively,



Calculation of the CEC from these structural formulae yields 1.09 meq/g (Stevens, 1945) and 0.66 meq/g (Köster, 1977). The measured CEC is 0.86 meq/g. Thus, the CEC value calculated from Stevens' formula is much too large. Furthermore, the two calculation methods result in different occupations of the tetrahedral and octahedral sheets. In extreme cases, a sample is classified as montmorillonite using Steven's (1945) calculation but is a beidellite using Köster's method, as illustrated by the following example:

The stoichiometric composition calculated for sample 4JUP by the methods of Stevens (1945) and Köster (1977) are, respectively,



The tetrahedral substitution according to Stevens (1945) was 49%, indicating a beidellitic montmorillonite, whereas Köster's method gave the value of 62%, indicating a montmorillonitic beidellite.

## STRUCTURE OF THE OCTAHEDRAL SHEET

Simultaneous thermal analysis is the best method for evaluating the structure of the octahedral sheet of turbostratic disordered smectites (Drits *et al.*, 1995; Drits, 2003; Wolters and Emmerich, 2007). The mass spectrometer curves of evolved water ( $m/e = 18$ ) during dehydroxylation were fitted and integrated peak areas of the identified peaks were calculated. The *cis*- and *trans*-vacant (*cv/tv*) proportions of these peak areas below and above 600°C of the smectites were calculated. Four classes of montmorillonites (*cv*, *cv/tv*, *tv/cv*, and *tv*) with respect to the distribution of the octahedral cations were distinguished (Wolters and Emmerich, 2007).

Most common are mixed *cv/tv* montmorillonites (ten samples) mainly with *cv* vacancies (74–50%). These samples can be divided into two subgroups, namely, samples with well-resolved peaks in the *tv* and *cv* region and samples with a broad shoulder below 600°C.

Pure *cv* montmorillonites (100% *cv* layers) are rare (six of nine *cv* samples). Even when classified as *cv* (Emmerich *et al.*, 2009), they contain up to 25% *tv* sites.

Four samples are *tv/cv* varieties. Samples with a main peak in the region above 600°C and a broad shoulder at lower temperatures were found in the *tv/cv* group. Continuous heating during STA measurements may lead to a broadening of the dehydroxylation peak and asymmetric shape (Guggenheim, 1990; Drits *et al.*, 1998). In this case, the *cv* proportions may be overestimated when the dehydroxylation curves are taken into account.

Samples with an Fe content >0.3 mol/f.u. showed a distinct peak in the *tv* region. With increasing amount of

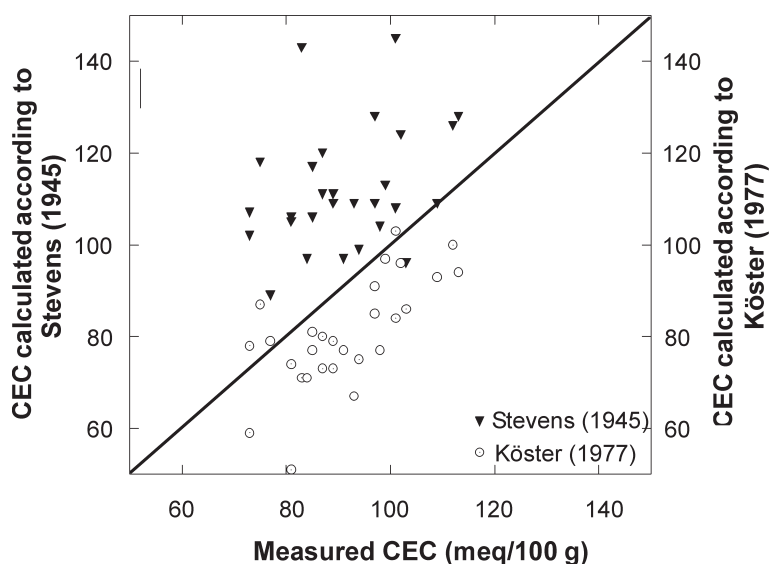


Figure 5. Discrepancies between measured and calculated CEC (meq/100 g) using the chemical formulae calculated according to Stevens (1945) and Köster (1977).

Table 9. Fields of different montmorillonites in ternary diagrams (mol/f.u.).

Montmorillonite	— Grim and Kulbicki (1961) —			——— Güven (1988) ———		
	Al	Mg	Fe <sup>3+</sup>	Al	Mg	Fe <sup>3+</sup>
Wyoming-type	>1.65	0.1–0.25	0.1–0.3	1.7–1.9	0.15–0.35	0.1–0.3
Cheto-type	1.25–1.6	0.35–0.65	<0.1	1.35–1.55	0.35–0.5	0.1–0.2

Fe, the proportions of the *tv* vacancies increased. Pure *tv* smectites should have at least 1.0 Fe mol/f.u. Iron ions reduce the thermal stability of 2:1 clay minerals due to the reduced bond energy Mg–OH > Al–OH > Fe–OH (Köster and Schwertmann, 1993). Five samples can be classified as *tv* but none is a pure *tv* montmorillonite.

To date, establishing whether the *cis*- and *trans*-vacancies are distributed within single octahedral sheets or smectites are composed of *cis*- and *trans*-vacant layers as in mixed-layer minerals has not been possible.

#### Relationships between structural properties

The structure of the octahedral sheet is characteristic of dioctahedral smectites. One purpose of the present study was to identify relationships between the ratio of *cis*- and *trans*-vacancies, the layer charge, the amount of Mg- and Fe-substitution, and the tetrahedral charge.

Ternary diagrams of the octahedral cation distribution were plotted by several authors to define different types of montmorillonite (Table 9). Grim and Kulbicki (1961) first computed the octahedral cation composition of montmorillonites and defined Wyoming-type, Cheto-type, and mixtures of Wyoming- and Cheto-type montmorillonites. Güven (1988) presented a compilation of literature data from Grim and Kulbicki (1961), Schultz (1969), Weaver and Pollard (1973), and Brigatti (1983).

According to Schultz (1969), low-charge smectites are defined by a layer charge of 0.2–0.375 eq/f.u. and high-charge samples are located in the 0.425–0.6 eq/f.u. region. Wyoming-type samples are low-charge montmorillonites; Cheto-type, high-charge.

Octahedral cation distributions derived from structural formulae lead to similar distributions (Figures 6, 7). Fields of low- and high-charge regions, such as Wyoming- and Cheto-type samples, cannot be distinguished. Low-, medium-, and high-charge montmorillonites/beidellites are distributed randomly in the ternary diagram on the basis of the calculated layer charge (Figure 6). According to the measured layer charge and the definition by Schultz (1969), all samples except one belong to low-charge smectites (Figure 7).

No relationship could be established between the proportion of *trans*-vacancies and layer charge, whether measured or calculated (Figure 8), nor was a correlation found between the Mg content and the octahedral structure (Figure 9a). *Cis*- and *trans*-vacancies vary insignificantly as a function of the Mg content.

McCarty and Reynolds (1995) found indirect proportionality among *cis*-vacancies and Fe<sup>3+</sup> content, and Mg substitution for Al in the octahedral sheets of mixed-layer illite-smectite minerals. With increasing degree of illitization, the Al content in the octahedral sheet

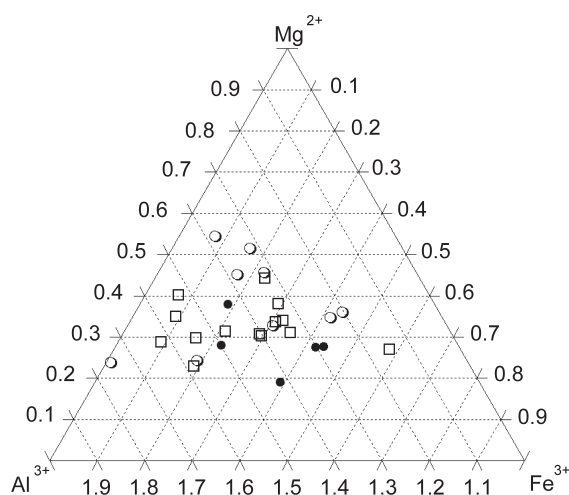


Figure 6. Octahedral cation distribution from the chemical formula calculated according to Stevens (1945). Layer charges derived from the formula after the classification of Schultz (1969): ● = 0.2–0.375, □ = 0.375–0.425, ○ = 0.425–0.6 (eq/f.u.).

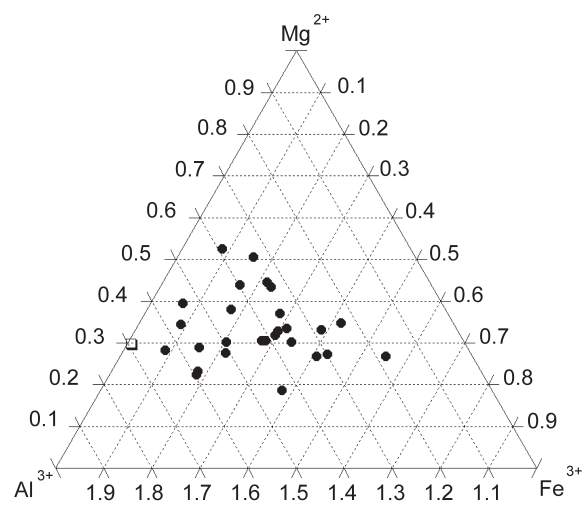


Figure 7. Octahedral cation distribution from the chemical formula as recommended by Köster (1977). Layer charges derived from alkylammonium exchange after the classification of Schultz (1969) with the following symbols for the charge domains: ● = 0.2–0.375, □ = 0.375–0.425.

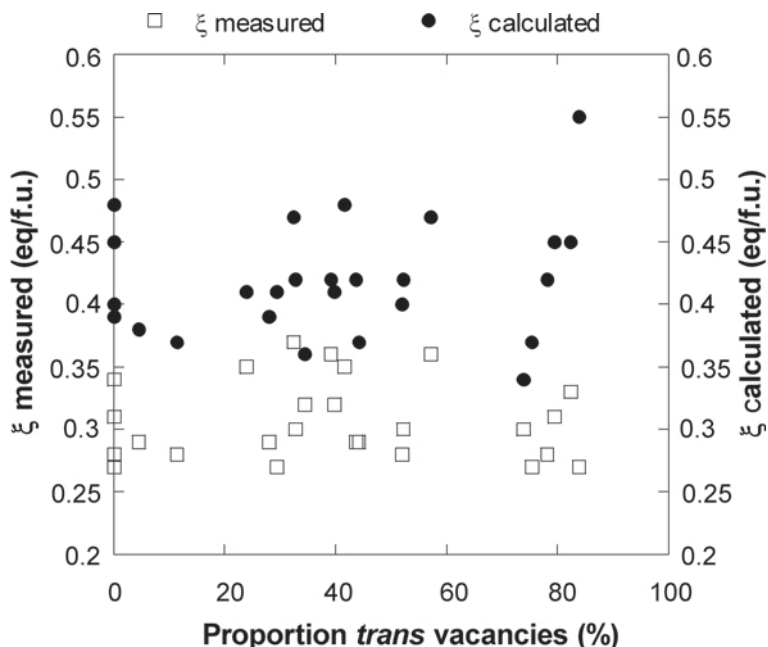


Figure 8. Calculated (from the structural formula of Stevens, 1945) and measured layer charge (alkylammonium exchange) related to *trans*-vacancies.

increased and the  $\text{Fe}^{3+}$  content decreased; thus, the proportion of *tv* increased. The  $\text{Fe}^{3+}$  ions segregate when the proportion of *tv* increases (McCarty and Reynolds, 1995).

The present results also show clearly that the relationship between *tv* sites and the Fe content of the octahedral sheet is very significant. A linear relationship was found between the octahedral Fe content and *trans*-vacant sites. The proportion of *tv* increased with the amount of  $^{\text{VI}}\text{Fe}^{3+}$ . The data show reasonable significance but the regression coefficient is  $\ll 1$  (Figure 9b).

Cuadros (2002) stated that Fe is associated with *cis*-sites in smectites.

The influence of Mg on the total layer charge is more important than on tetrahedral charge. The  $^{\text{IV}}\text{Al}$  content, *i.e.* the tetrahedral charge, has a tendency to increase with decreasing amount of  $^{\text{VI}}\text{Mg}$  (Figure 10a).

The number of Fe ions and the tetrahedral charge are also correlated (Figure 10b). The  $^{\text{IV}}\text{Al}$  content increases with the amount of  $^{\text{VI}}\text{Fe}^{3+}$ . The substitution of  $\text{Fe}^{3+}$  in the octahedral sheet and Al in the tetrahedral sheet is conceivable due to the ionic radii. The larger  $\text{Fe}^{3+}$  ions

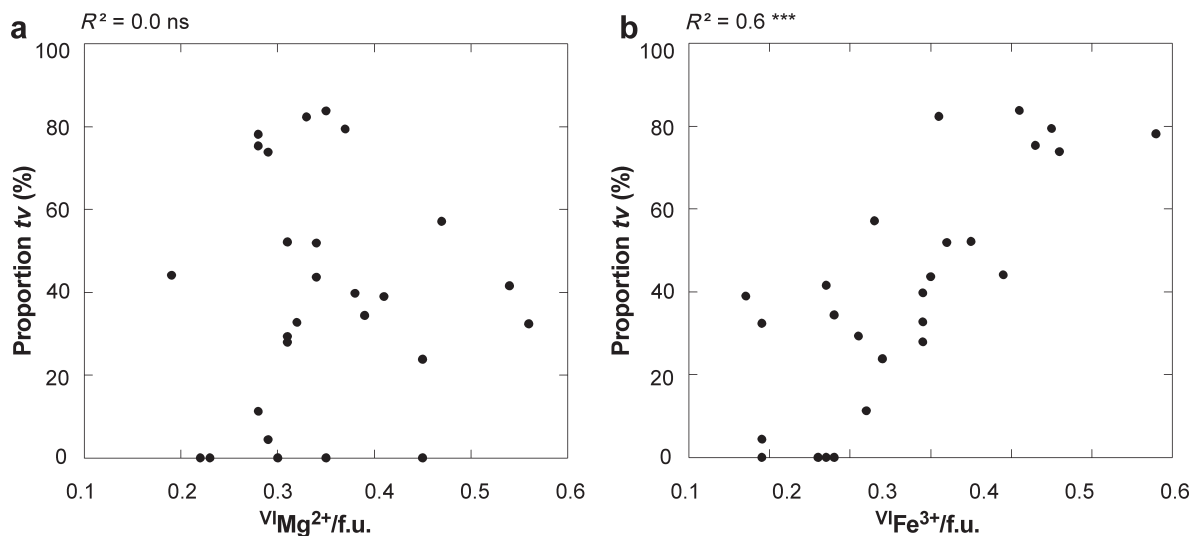


Figure 9. Mg content (a) and  $^{\text{VI}}\text{Fe}^{3+}$  (b) related to *trans*-vacancies.

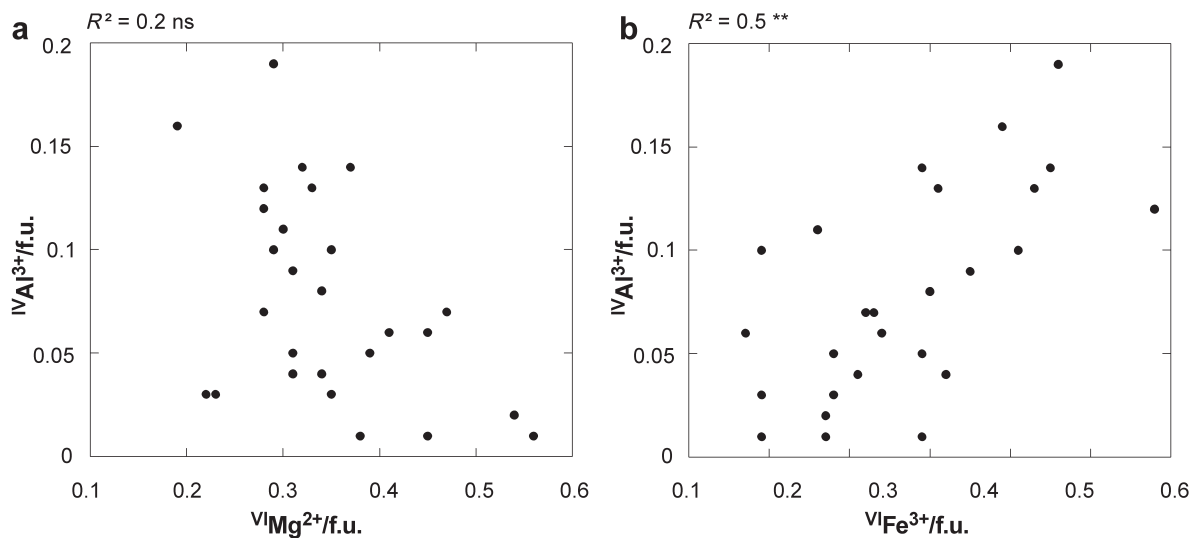


Figure 10. Mg content (a) and  $^{VI}Fe^{3+}$  (b) related to tetrahedral charge (expressed as  $^{IV}Al^{3+}/f.u.$ ).

(ionic radius 63 pm) would cause stronger distortions in the tetrahedral sheet than Al (53 pm). Mössbauer spectra indicated the absence of Fe ions in the tetrahedral sheet (Wolters, 2005).

Bishop *et al.* (2002) investigated the influence of octahedral and tetrahedral cation substitution on the structure of smectites and serpentines by infrared spectroscopy. Tetrahedral substitution of Al or  $Fe^{3+}$  for Si is expected to disrupt the general dioctahedral structure and influence the octahedral sheet due to changes in cation size and charge (Table 10).

Sainz-Diaz *et al.* (2004) simulated variations of the tetrahedral charge and demonstrated that these variations result in slight differences in the cation distribution. Those authors focused on Fe clustering but failed to establish a relationship between the tetrahedral charge and Fe content. Literature reports disagree as to the clustering of Fe ions. Based on experimental and computational methods, Besson *et al.* (1987), Drits *et al.* (1997), Sainz-Diaz *et al.* (2004), and Vantelon *et al.* (2003) argued in favor of Fe clustering. Manceau *et al.* (2000) investigated reduced nontronites and found that the cluster distribution of Fe between *cis*- and *trans*-octahedral sites changed upon reduction of structural Fe from Fe(III) to Fe(II).

The tetrahedral charge was also positively correlated with *trans*-vacancies (Figure 11a) in the present sample

Table 10. Ionic radii (pm) of tetrahedral and octahedral cations (Huheey *et al.*, 1993).

Ionic radii	$Si^{4+}$	$Al^{3+}$	$Fe^{3+}$	$Mg^{2+}$
Tetrahedral sheet (IV)	40	53	63	—
Octahedral sheet (VI)	—	68	69	86

series. In contrast, Drits *et al.* (1997) postulated that no correlation between the dehydroxylation temperature and tetrahedral charge exists for 2:1 clay minerals. Tunega *et al.* (2007) calculated that a *cis*-coordination of hydroxyl groups around octahedral vacancies is more stable in the presence of tetrahedral substitutions. For the  $Na^+$ -saturated,  $<2 \mu m$  fractions of beidellites from the Black Jack Mine and Boddington, Singh and Gilkes (1991) suggested beidellite dehydroxylation temperatures of 510–530°C, corresponding to *tv* varieties. These results are in agreement with those of Tshipursky and Drits (1984) who found that beidellite tends to be *tv* while montmorillonite tends to be mainly *cv*. The Unterrupsroth beidellite (24Beid) is a *cv* variety, although its tetrahedral charge should promote *trans*-vacancies – this beidellite, however, seems to be exceptional. The relationship between tetrahedral charge and *trans*-vacancies is likely restricted to montmorillonites.

Cuadros (2002) investigated the *b* dimension in smectites and the lateral dimension of the octahedral and tetrahedral sheets. Due to cation-size effects, the octahedral *b* dimensions are smaller than the tetrahedral *b* dimensions. Cuadros (2002) concluded, when correlating the ideal *b* parameters of octahedral and tetrahedral sheets, that an increase in  $^{IV}Al$  causes an increase in octahedral  $Mg + Fe^{3+}$  and *vice versa*. Cuadros (2002) states that a *cv* sheet has a smaller *b* dimension than a *tv* sheet. When the tetrahedral sheets have low substitutions and, therefore, a smaller lateral dimension, a *cv* sheet is preferred.

The dominant factor, which is related to the tetrahedral charge, is the  $Fe^{3+}$  content. Positive correlation exists between the octahedral cations ( $Mg + Fe^{3+}$ ) and  $^{IV}Al$  (Figure 11b), even if Mg is negatively correlated with  $^{IV}Al$  (Figure 10a).

In Figure 12 the cation distribution is plotted *vs.* the tetrahedral substitution. All samples with  $\text{Fe}^{3+} < 0.3$  mol/f.u. have tetrahedral substitution of  $< 10\%$ .

A plot of the octahedral cation distribution combined with the proportion of *cv/tv* indicates that samples with 10–50% of tetrahedral substitution and *cis*- and *trans*-vacancies are randomly distributed (Figure 13). Samples with 0–10% tetrahedral charge are situated in the field below  $< 0.3 \text{ Fe}^{3+}$  mol/f.u. Thus, the cation distribution, in combination with the octahedral structure, supports the borderline 0.3 mole  $\text{Fe}(\text{III})/\text{f.u.}$  detected by Brigatti (1983). At greater Fe contents, the smectites are *trans*-vacant, and below this value, *cis*-vacant. This indicates that the Fe content controls the kind of octahedral structure. The 0.3 mol/f.u. of Fe value appears to be the boundary between the octahedral structure (*cv/tv*) and the tetrahedral substitution.

Thus, smectites with  $\text{Al} > 1.4$  mol/f.u. and  $\text{Fe}^{3+} < 0.3$  mol/f.u. are *cis*-vacant and those with  $\text{Al} < 1.4$  mol/f.u. and  $\text{Fe}^{3+} > 0.3$  mol/f.u. are *trans*-vacant.

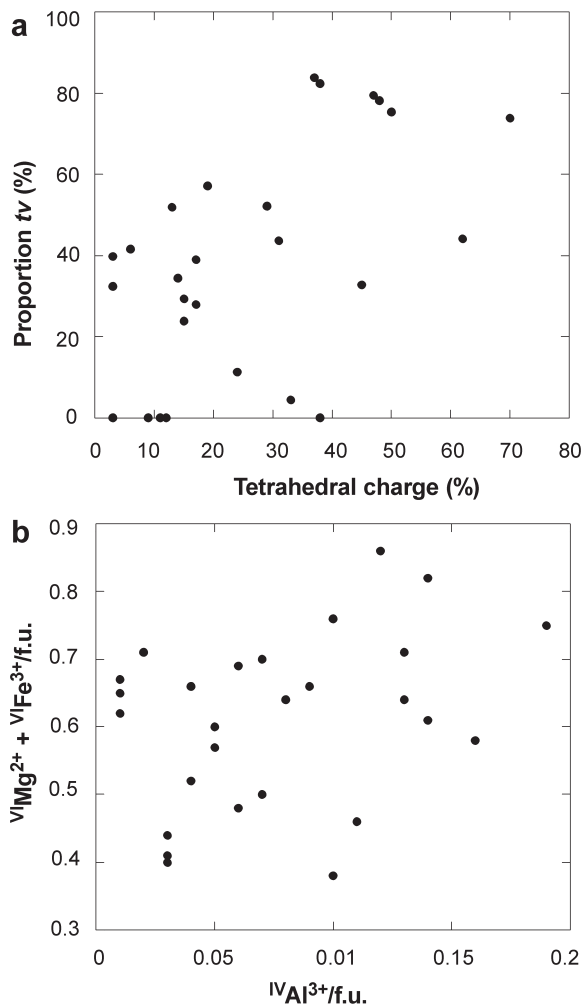


Figure 11. Tetrahedral charge related to *trans*-vacancies (a) and  $\text{IV Al}^{3+}$  related to octahedral cations  $\text{Mg}^{2+} + \text{Fe}^{3+}$  (b).

Brigatti (1983) designated montmorillonites to be Fe-rich if 15–30% of their octahedral cations were Fe and classified nontronites to be those smectites in which  $> 75\%$  of the octahedral cations is Fe. In contrast, Güven (1988) proposed setting the boundary between montmorillonite and nontronite at 50% Fe. According to Güven (1988), a miscibility gap exists between montmorillonite and nontronite, the existence of which has promoted some controversy in the literature: Meunier (2005) pointed out that the *b*-cell dimensions of beidellite and nontronite are too different to allow a continuous series. According to Köster *et al.* (1999), no complete solid-solution is indicated between montmorillonite and beidellite. Recent studies, however, do favor a continuous series. Therefore, the range of 15–30% (0.3–0.6 mol/f.u.) octahedral Fe should not be used for a classification system. The present authors prefer, assuming no miscibility gap, the IMA rules in combination with the proven borderline of 15%  $\text{VI Fe}^{3+}$  (0.3 mol/f.u.). Smectites with an Fe content of 15–50% (0.3–1.0 mol/f.u.) are classified as ferrian smectites.

The present results, in combination with data from the literature, argue persuasively that no miscibility gap exists between montmorillonites, beidellites, and nontronites. According to Gaudin *et al.* (2004b), a chemical continuity exists between nontronite and the so-called ‘Fe-montmorillonite’ end-members. Montmorillonites are very abundant in nature whereas nontronites are rare. Bishop *et al.* (2002), Brigatti (1983), Gaudin *et al.* (2004a, 2004b), Köster *et al.* (1999), Madejová *et al.* (2000), and Mayayo *et al.* (2000) investigated Fe-containing smectites ranging from montmorillonites to nontronites. The ternary system  $\text{Al}_2$ ,  $\text{Mg}_2$ , and  $\text{Fe}_2^{3+}$  shows a continuous substitution of Al for Fe, or *vice versa*, for dioctahedral smectites as revealed by the octahedral cation distributions from the above results

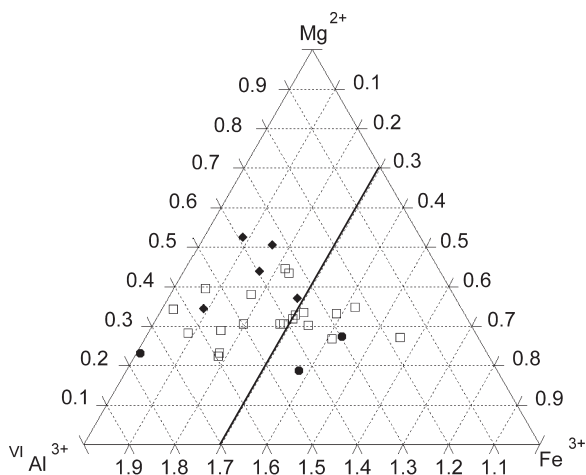


Figure 12. Octahedral cation distribution calculated according to Köster (1977) and  $\text{IV Al}^{3+}$  substitution with the following regions:  $\blacklozenge$  = 0–10%,  $\square$  = 11–50%,  $\bullet$  = 51–90%.

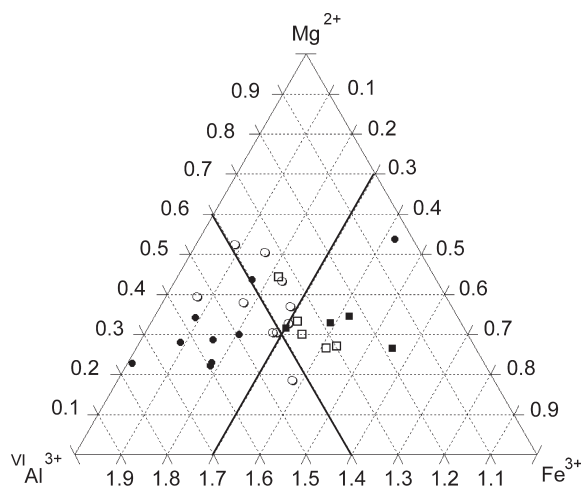


Figure 13. Octahedral cation distribution calculated according to Köster (1977) and *cis*- and *trans*-vacancies with the following regions:  $\blacklozenge$  =  $w_{cv}$  24–0%/  $w_{tv}$  76–100%,  $\square$  =  $w_{cv}$  49–25%/  $w_{tv}$  51–75%,  $\circ$  =  $w_{cv}$  49–25%/  $w_{tv}$  51–75%,  $\bullet$  =  $w_{cv}$  100–75%/  $w_{tv}$  0–25%.

(Figure 14). Petit *et al.* (2002) investigated, in a heterogeneous Fe-smectite sample, two different populations, which may occur either as separate particles or possibly also as interstratified layers. Two types of montmorillonites were distinguished: one population with a large  $\text{Fe}^{3+}$  content contained little or no tetrahedral charge and an intermediate species with a tetrahedral charge. The intermediate form was between nontronite (dominant tetrahedral charge) and montmorillonite (dominant octahedral charge). As a major difference between montmorillonite and nontronite, tetrahedral substitution by Fe ions only occurs in nontronite (Bishop *et al.*, 1999; Goodman *et al.*, 1976). The present results also reveal that montmorillonites have no substitutions of  $\text{Fe}^{3+}$  for Si. The occurrence of Fe in tetrahedral sites is probably restricted to nontronites.

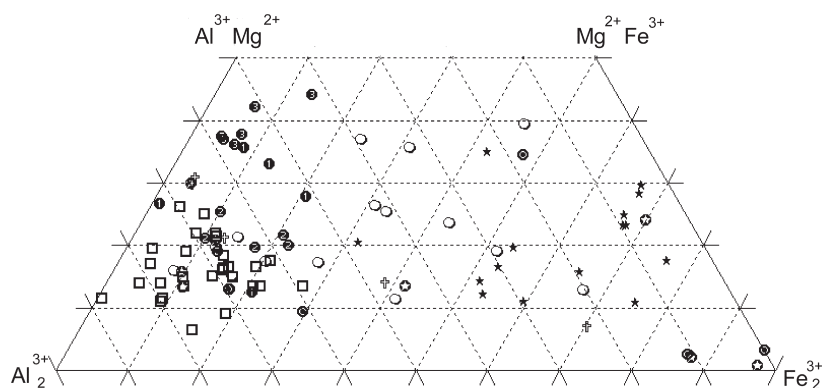


Figure 14. Octahedral cation distribution of  $\text{Al}_2^{3+}$ ,  $\text{Mg}_2$  and  $\text{Fe}_2^{3+}$  showing a continuous series between montmorillonites and nontronites.

## CONCLUSIONS

(1) Comprehensive characterization of 28 smectites (Na-saturated,  $<0.2 \mu\text{m}$ ) reveals wide ranges in the chemistry, structure, layer charge, and location of charge of montmorillonites.

(2) Dioctahedral 2:1 clay minerals identified as members of the montmorillonite-beidellite series can be described unambiguously by their layer charge, the amount of tetrahedral charge, the arrangement of the octahedral cations, and the Fe content.

(3) An appropriate calculation of the stoichiometric elemental composition is the most important task for achieving a reliable characterization. The essential work of Köster (1977), who integrated the measured layer charge into the calculation of the chemical formula, is still often ignored in the literature. The layer charge derived from chemical analyses according to Stevens (1945) can be greater, by up to 0.2 eq/f.u., than the independently-measured layer charge (alkylammonium method). Using Köster's (1977) method, the CEC values calculated from the stoichiometric formula are consistent with the measured CEC values. The calculated CEC values are, because of the pH-dependent charge of the edges, mostly 10 to 20% less than the measured values. In contrast, the CEC values according to Stevens' formula are, in general, distinctly larger than the measured values.

(4) Among the dioctahedral smectites selected, the variation in layer charge is very limited compared to the published variation for montmorillonites/beidellites.

(5) Simultaneous thermal analysis is the best method for evaluating the structure of the octahedral sheet of turbostratically disordered smectites. Maxima of the dehydroxylation temperatures below or above  $600^\circ\text{C}$  allow discrimination of *tv* and *cv* sites.

(6) The results indicate relationships among the amount of Fe ions, the location of charge, and the dehydroxylation temperature.

(7) No relationship was established between the total layer charge and the proportion of *trans*-vacancies in the octahedral sheet.

(8) The Mg content is not correlated with the octahedral structure. *Cis*- and *trans*-vacancies do not vary significantly as a function of the Mg content.

(9) The present results demonstrate that the Fe content is the dominant factor controlling the octahedral-sheet structure. The number of *trans*-vacancies increases with Fe content. Samples with an Fe content of >0.3 mol/f.u. are dominantly *tv* and those with Fe<sup>3+</sup> <0.3 mol/f.u. are *cv* varieties.

(10) The Fe content also influences the tetrahedral substitution. Both the <sup>IV</sup>Al content and the proportion of *trans*-vacancies increase with the amount of <sup>VI</sup>Fe<sup>3+</sup>. Thus, tetrahedral substitution is also a function of the number of *trans*-vacancies. Such a relationship is likely restricted to smectites, especially to montmorillonites.

#### ACKNOWLEDGMENTS

The authors greatly appreciate the partial financial support of the project by the Federal Institute for Geosciences and Natural Resources (BGR), Hannover, Germany. Many samples were supplied by Dr R. Ahlers (Stüd Chemie AG) and Prof. Dr M.F. Brigatti (University of Modena). The authors thank Annett Steudel and Kyra Seibert for their help in the laboratory and Frank Korte and Detlef Requard (BGR) for the XRF analyses. They are also grateful to Peter Weidler, Andreas Bauer (INE, FZKA), Bruno Lanson (CNRS, Grenoble), Stefan Kaufhold (BGR), Michael Plötze (ETH Zurich), and Marian Janek (Comenius University, Bratislava) for their constructive criticism of the work. They thank Ursel and Fritz Wagner (München) and Heike Reuter (FZKA) for the Mössbauer spectroscopy measurements. Finally, the authors are grateful to Helge Stanjek (RWTH Aachen) for his constructive comments, which improved the manuscript.

#### REFERENCES

- Ammann, L., Bergaya, F., and Lagaly, G. (2005) Determination of the cation exchange capacity of clays with copper complexes revisited. *Clay Minerals*, **40**, 441–453.
- Bain, D.C. and Smith, B.F.L. (1992) Chemical analysis. Pp. 300–322 in: *Clay Mineralogy: Spectroscopic and Chemical Determinative Methods* (M.J. Wilson, editor). Chapman & Hall, London.
- Bergaya, F., Lagaly, G., and Vayer, M. (2006) Cation and anion exchange. Pp. 979–1001 in: *Handbook of Clay Science* (F. Bergaya, B.K.G. Theng, and G. Lagaly, editors). Elsevier Amsterdam.
- Besson, G., Drits, V.A., Daynyak, L.G., and Smoliar, B.B. (1987) Analysis of cation distribution in dioctahedral micaceous minerals on the basis of IR spectroscopy data. *Clay Minerals*, **22**, 465–478.
- Bishop, J.L., Murad, E., and Dyar, M.D. (2002) The influence of octahedral and tetrahedral cation substitution on the structure of smectites as observed through infrared spectroscopy. *Clay Minerals*, **37**, 617–628.
- Brigatti, M.F. (1983) Relationship between composition and structure in Fe-rich smectites. *Clay Minerals*, **18**, 177–186.
- Brigatti, M.F. and Poppi, L. (1981) A mathematical model to distinguish the members of the dioctahedral smectite series. *Clay Minerals*, **16**, 81–89.
- Carrado, K.A., Decarreau, A., Petit, S., Bergaya, F., and Lagaly, G. (2006) Synthetic clay minerals and purification of natural minerals. Pp. 115–139 in: *Clay Mineralogy: Spectroscopic and Chemical Determinative Methods* (M.J. Wilson, editor). Chapman & Hall, London.
- Christidis, G.E. and Eberl, D.D. (2003) Determination of layer-charge characteristics. *Clays and Clay Minerals*, **51**, 644–655.
- Cuadros, J. (2002) Structural insights from the study of Cs-exchanged smectites submitted to wetting and drying cycles. *Clay Minerals*, **37**, 473–486.
- Dohrmann, R. (1999) Aufbereitung der Tonminerale - Von der Probe zum Präparat In 2. *European Workshop on Clay Mineralogy* (A. Bauer, editor). Jena, 15 pp.
- Drits, V.A. (2003) Structural and chemical heterogeneity of layer silicates and clay minerals. *Clay Minerals*, **38**, 403–432.
- Drits, V.A., Besson, G., and Muller, F. (1995) An improved model for structural transformations of heat-treated aluminous dioctahedral 2:1 layer silicates. *Clays and Clay Minerals*, **43**, 718–731.
- Drits, V.A., Dainyak, L.G., Muller, F., Besson, G., and Manceau, A. (1997) Isomorphous cation distribution in celadonites, glauconites and Fe-illites determined by infrared, Mössbauer and EXAFS spectroscopies. *Clay Minerals*, **32**, 153–179.
- Drits, V.A., Lindgreen, H., Salyn, A.L., Ylagan, R., and McCarty, D.K. (1998) Semiquantitative determination of *trans*-vacant and *cis*-vacant 2:1 layers in illites and illite-smectites by thermal analysis and X-ray diffraction. *American Mineralogist*, **83**, 1188–1198.
- Emmerich, K. (2000) Die geotechnische Bedeutung des Dehydroxilierungsverhaltens quellfähiger Tonminerale. PhD thesis, ETH, Zürich, 135 pp.
- Emmerich, K., Wolters, F., Kahr, G., and Lagaly, G. (2009) Clay profiling: the classification of montmorillonites. *Clays and Clay Minerals*, **53**, 104–114.
- Gaudin, A., Grauby, O., Noack, Y., Decarreau, A., and Petit, S. (2004a) The accurate crystal chemistry of ferric smectites from the lateritic nickel ore of Murrin Murrin (Western Australia). I. XRD and multi-scale approaches. *Clay Minerals*, **39**, 301–316.
- Gaudin, A., Petit, S., Rose, J., Martin, F., Decarreau, A., Noack, Y., and Borschneck, D. (2004b) The accurate crystal chemistry of ferric smectites from the lateritic nickel ore of Murrin Murrin (Western Australia). II. Spectroscopic (IR and EXAFS) approaches. *Clay Minerals*, **39**, 453–467.
- Goodman, B.A., Russell, J.D., Fraser, A.R., and Woodhams, F.W.D. (1976) A Mössbauer and IR spectroscopy study of the structure of nontronite. *Clays and Clay Minerals*, **24**, 53–59.
- Grim, R.E. and Kulbicki, G. (1961) Montmorillonite: High temperature reactions and classification. *American Mineralogist*, **46**, 1329–1369.
- Guggenheim, S. (1990) The dynamics of thermal decomposition in aluminous dioctahedral 2:1 layer silicates: A crystal chemical model. *9th International Clay Conference*, **2**, 99–107, Strasbourg, France.
- Güven, N. (1988) Smectites. Pp. 497–552 in: *Hydrous Phyllosilicates* (S.W. Bailey, editor). Reviews in Mineralogy, **19**, Mineralogical Society of America, Washington, D.C.
- Huheey, J.E., Keiter, E.A., and Keiter R.L. (1993) *Inorganic Chemistry: Principles of Structure and Reactivity*. Harper Collins, New York.
- Jasmund, K. and Lagaly, G. (editors) (1993) *Tonminerale und Tone*. Steinkopff Verlag, Darmstadt, Germany.
- Kaufhold, S., Dohrmann, R., Ufer, K., and Meyer, F.M. (2002) Comparison of methods for the quantification of montmor-

- illonite in bentonites. *Applied Clay Science*, **22**, 145–151.
- Köster, H.M. (1977) Die Berechnung kristallchemischer Strukturformeln von 2:1 – Schichtsilikaten unter Berücksichtigung der gemessenen Zwischenschichtladungen und Kationenumtauschkapazitäten, sowie der Darstellung der Ladungsverteilung in der Struktur mittels Dreieckskoordinaten. *Clay Minerals*, **12**, 45–54.
- Köster, H.M. and Schwertmann, U. (1993) Dreischichtminerale. Pp. 33–58 in: *Tonminerale und Tone* (K. Jasmund and G. Lagaly, editors). Steinkopff Verlag, Darmstadt, Germany.
- Köster, H.M., Ehrlicher, U., Gilg, H.A., Jordan, R., Murad, E., and Onnich, K. (1999) Mineralogical and chemical characteristics of five nontronites and Fe-rich smectites. *Clay Minerals*, **34**, 579–599.
- Lagaly, G. (1989) Erkennung und Identifizierung von Tonmineralen mit organischen Stoffen *Jahrestagung der DTTG 1989*, pp. 86–129.
- Lagaly, G. (1994) Layer charge determination by alkylammonium ions. Pp. 1–46 in: *Layer Charge Characteristics of 2:1 Silicate Clay Minerals* (A.R. Mermut, editor). Workshop Lectures volume 6, The Clay Minerals Society, Boulder, Colorado, USA.
- Lagaly, G. and Weiss, A. (1971) Anordnung und Orientierung kationischer Tenside auf ebenen Silicatoberflächen Teil IV. *Kolloid-Zeitschrift und Zeitschrift für Polymere*, **243**, 48–55.
- Laird, D.A., Scott, A.D., and Fenton, T.E. (1989) Evaluation of the alkylammonium method of determining layer charge. *Clays and Clay Minerals*, **37**, 41–46.
- Madejová, J., Bujdák, J., Petit, S., and Komadel, P. (2000) Effects of chemical composition and temperature of heating on the infrared spectra of Li-saturated dioctahedral smectites. (I) Mid-infrared region. *Clay Minerals*, **35**, 739–751.
- Manceau, A., Drits, V., Lanson, B., Chateigner, D., Wu, J., Huo, D., Gates, W.P., and Stucki, J.W. (2000) Oxidation-reduction mechanism of iron in dioctahedral smectites. II. Crystal chemistry of reduced Garfield nontronite. *American Mineralogist*, **85**, 153–172.
- Martin, R.T., Bailey, S.W., Eberl, D.D., Fanning, D.S., Guggenheim, S., Kodama, H., Pevear, D.R., Šrodoň, J., and Wicks, F.J. (1991) Report of The Clay Minerals Society nomenclature committee: Revised classification of clay materials. *Clays and Clay Minerals*, **39**, 333–335.
- Mayayo, M.J., Bauluz, B., and Gonzalez Lopez, J.M. (2000) Variations in the chemistry of smectites from the Calatayud Basin (NE Spain). *Clay Minerals*, **35**, 365–374.
- Mehra, O.P. and Jackson, M.L. (1960) Iron oxide removal from soils and clays by a dithionite-citrate-system buffered with sodium bicarbonate. Pp. 317–327 in the *7th National conference on Clays and Clay Minerals* (A. Swineford, editor). Pergamon Press, Washington, D.C.
- Meier, L.P. and Kahr, G. (1999) Determination of the cation exchange capacity (CEC) of clay minerals using the complexes of copper (II) ion with triethylenetetramine and tetraethylenepentamine. *Clay and Clay Minerals*, **47**, 386–388.
- Meunier, A. (2005) *Clays*. Springer, Berlin.
- Olis, A.C., Malla, P.B., and Douglas, L.A. (1990) The rapid estimation of the layer charges of 2:1 expanding clays from a single alkylammonium ion expansion. *Clay Minerals*, **25**, 39–50.
- Petit, S., Caillaud, J., Righi, D., Madejová, J., Elsass, F., and Köster, H.M. (2002) Characterization and crystal chemistry of an Fe-rich montmorillonite from Ölberg, Germany. *Clay Minerals*, **37**, 283–297.
- Rühlicke, G. and Kohler, E.E. (1981) A simplified procedure for determining layer charge by the n-alkylammonium method. *Clay Minerals*, **16**, 305–307.
- Sainz-Diaz, C.I., Palin, E.J., Hernández-Laguna, A., and Dove, M.T. (2004) Effect of the tetrahedral charge on the order-disorder of the cation distribution in the octahedral sheet of smectites and illites by computational methods. *Clays and Clay Minerals*, **52**, 357–374.
- Schultz, L.G. (1969) Lithium and potassium absorption, dehydroxylation temperature and structural water content of aluminous smectites. *Clays and Clay Minerals*, **17**, 115–149.
- Singh, B.S. and Gilkes, R.J. (1991) A potassium rich beidellite from a laterite pallid zone in Western Australia. *Clay Minerals*, **26**, 233–244.
- Stevens, R.E. (1945) A system for calculating analyses of micas and related minerals to end members. *U.S. Geological Survey Bulletin*, **950**, 101–119.
- Tributh, H. and Lagaly, G.A. (1986a) Aufbereitung und Identifizierung von Boden- und Lagerstättentonen. I. Aufbereitung der Proben im Labor In *GIT Fachzeitschrift für das Laboratorium*, **30**, 524–529.
- Tributh, H. and Lagaly, G.A. (1986b) Aufbereitung und Identifizierung von Boden- und Lagerstättentonen. II. Korngrößenanalyse und Gewinnung der Tonsubfraktion In *GIT Fachzeitschrift für das Laboratorium*, **30**, 771–776.
- Tsipursky, S.I. and Drits, V.A. (1984) The distribution of octahedral cations in the 2:1 layers of dioctahedral smectites studied by oblique texture electron diffraction. *Clay Minerals*, **19**, 177–192.
- Tunega, D., Goodman, B.A., Haberhauer, G., Reichenauer, T.G., Gerzabek, M.H., and Lischka, H. (2007) *Ab initio* calculations of relative stabilities of different structural arrangements in dioctahedral phyllosilicates. *Clays and Clay Minerals*, **55**, 220–232.
- Ufer, K., Roth, G., Kleeberg, R., Stanjek, H., Dohrmann, R., and Bergmann, J. (2004) Description of X-ray powder pattern of turbostratically disordered layer structures with a Rietveld compatible approach. *Zeitschrift für Kristallographie*, **219**, 519–527.
- van Olphen, H. (1963) *An Introduction to Clay Colloid Chemistry*. Interscience Publisher, New York.
- Vantelon, D., Montarges-Pelletier, E., Michot, L.J., Briois, V., Pelletier, and Thomas, F. (2003) Iron distribution in the octahedral sheet of dioctahedral smectites. An Fe-K-edge X-ray absorption spectroscopy study. *Physics and Chemistry of Minerals*, **30**, 44–53.
- Vogt, K. and Köster, H.M. (1978) Zur Mineralogie, Kristallchemie und Geochemie einiger Montmorillonite aus Bentoniten. *Clay Minerals*, **13**, 25–43.
- Wagner, F.E. and Kyek, A. (2004) *Mössbauer Spectroscopy in Archeology: Introduction and Experimental Considerations*. Kluwer Academic Publishers, Dordrecht, The Netherlands.
- Weaver, C.E. and Pollard, L.D. (1973) *The Chemistry of Clay Minerals*. Developments in Sedimentology, **15**, Elsevier Scientific Publishers, Amsterdam
- Wolters, F. (2005) Classification of Montmorillonites. PhD thesis, Universität Karlsruhe, Germany, 98 pp.
- Wolters, F. and Emmerich, K. (2007) Thermal reactions of smectites – relation of dehydroxylation temperature to octahedral structure. *Thermochimica Acta*, **462**, 80–88.

(Received 11 January 2008; revised 22 November 2008; Ms. 0117; A.E. J.D. Fabris)